

Account/Revue

“Chimie douce”: A land of opportunities for the designed construction of functional inorganic and hybrid organic-inorganic nanomaterials

C. Sanchez^{*}, L. Rozes, F. Ribot, C. Laberty-Robert,
D. Grosso, C. Sassoie, C. Boissiere, L. Nicole

UMR CNRS 7574, Chimie de la matière condensée de Paris, université Paris 6 (UPMC),
Collège de France, bâtiment C–D, 11, place Marcelin-Berthelot, 75231 Paris, France

Received 14 April 2009; accepted after revision 2 June 2009

Available online 17 July 2009

Abstract

“Chimie douce” based strategies allow, through the deep knowledge of materials chemistry and processing, the birth of the molecular engineering of nanomaterials. This feature article will highlight some of the main research accomplishments we have performed during the last years. We describe successively the design and properties of: sol–gel derived hybrids, Nano Building Blocks (NBBs) based hybrid materials, nanostructured porous materials proceeds as thin films and ultra-thin films, aerosol processed mesoporous powders and finally hierarchically structured materials. The importance of the control of the hybrid interfaces via the use of modern tools as DOSY NMR, SAXS, WAXS, Ellipsometry that are very useful to evaluate in situ the hybrid interfaces and the self-assembly processes is emphasized. Some examples of the optical, photocatalytic, electrochemical and mechanical properties of the resulting inorganic or hybrid nanomaterials are also presented. **To cite this article:** C. Sanchez et al., *C. R. Chimie* 13 (2010).

© 2009 Published by Elsevier Masson SAS on behalf of Académie des sciences.

Keywords: Hybrid; Nanomaterials; Mesoporous; Photocatalysis; Fuel cells; Sensors; Hierarchical structures

1. Introduction

In all living organisms nature provides a multiplicity of materials (organic, inorganic, hybrids and composites), architectures, systems and functions. Natural composites, such as mollusk shells or crustacean carapaces and in the human body, bone or tooth tissues, are characterized by hierarchical constructions at scales ranging from nanometers, micrometers, to

millimeters that introduce the capacity to answer the physical or chemical demands occurring at these different levels [1–4]. Indeed, many natural materials are highly integrated hybrid systems synthesized in mild chemical conditions and have found the best compromise between different properties or functions (mechanics, density, permeability, colour, hydrophobia...). Such highly complex and aesthetic structures pass well beyond current man-made materials accomplishments.

Maya blue is a beautiful example of a very old and remarkable man-made hybrid material processed via soft chemical conditions. It is a synergic material that

^{*} Corresponding author.

E-mail address: clement.sanchez@upmc.fr (C. Sanchez).

combines the color of the organic pigment (*indigo*) and the resistance of the inorganic host (*clay mineral known as palygorskite*), with properties and performance well beyond those of a simple mixture of its components. But as for many other ancient materials, its conception was most likely the fruit of a fortunate accident, an ancient serendipitous discovery [5].

More than twelve centuries later, our refined analytical techniques have allowed us to understand the true nature and atomic and molecular structure of many materials. In the 1970s, the concept of “chimie douce” pioneered by Livage [6–8] opened up a new “école de pensée”. The controlled design of novel advanced inorganic or hybrid materials was born replacing the trial and error tradition.

Indeed “chimie douce” based strategies allow, through the deep knowledge of materials chemistry and processing, the birth of the molecular engineering of nanomaterials [7,9–14]. Today with the recent advances made in the field of materials chemistry the “biomimetic and bioinspired” chemical construction and patterning of materials with long-range order architectures (beyond nanometer size) is an important scientific and technological challenge which becomes accessible [11,15–17].

For many years the “Hybrid Materials group” of the Laboratoire chimie de la matière condensée de Paris at the University Pierre et Marie Curie has been working on the field of “chimie douce” based construction of advanced materials and related areas (hybrids and nanomaterials, organized matter chemistry, integrative chemistry. . .). The interested reader will find in the following set of comprehensive reviews the different research topics explored by the group [9–11,15,18–22].

The present feature article will highlight some of the main research accomplishments we have performed during the last years. Indeed, through a few selected examples we try to demonstrate that “chimie douce” has opened a land of opportunities for the designed construction of functional inorganic and hybrid organic-inorganic nano materials. After a brief reminder of the chemical background and general synthesis strategies we will describe:

- the sol–gel derived hybrids that will be compared to the hybrid designed through the Nano Building Blocks (NBBs) approaches;
- the elaboration of nanostructured porous materials proceeds as thin films and ultra-thin films;
- the synthesis of aerosol processed mesoporous powders and hierarchically structured materials.

We will emphasise the importance of the control of the hybrid interfaces to be able to tailor made nanomaterials. In this context tools as DOSY NMR, SAXS, Ellipsometry, etc. are very useful to evaluate in situ the hybrid interfaces and the self-assembly processes. These comprehensive studies are very important to design functional hybrid materials. Some examples of the optical, photocatalytic, electrochemical and mechanical properties of the resulting inorganic or hybrid nanomaterials will also be presented and briefly discussed.

2. Hybrid materials and sol–gel chemistry: general background

Hybrid inorganic-organic materials can be broadly defined as synthetic materials with organic and inorganic components, intimately mixed. Such materials could be either homogeneous derived from monomers and miscible organic and inorganic components, or heterogeneous and phase-separated where at least one of the component domains has a dimension ranging from few Å to several nanometers [7,23,24]. Hybrid nanocomposites had an explosive development since the 1980s, with the expansion of soft inorganic chemistry processes. The mild synthetic conditions provided by the sol–gel process such as metallo-organic precursors, low processing temperatures and the versatility of the colloidal state allow for the mixing of the organic and inorganic components at the nanometer scale in virtually any ratio [9,10,14,19,25].

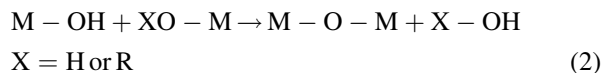
2.1. Sol–gel chemistry in brief

Sol–gel chemistry is central in the development of hybrid materials. Typically, $M(OR)_n$, MX_n , $R'-M(OR)_{n-1}$ precursors are commonly used, where M represents a metal center, n is its oxidation state and X and RO are common “leaving groups” present in metallic salts or metal alkoxides. X can for example represent a chloride anion, as in metal halides. R' is any organic functionality anchored to the metallic center via covalent bonds ($Si-C$, $Sn-C$) or via complexing ligands ($M = Ti, Zr, \dots$). The sol–gel process implies connecting the metal centers with oxo- or hydroxo- bridges, therefore generating metal-oxo or metal-hydroxopolymer in solution. *Hydrolysis* of an alkoxy group or deprotonation of a water molecule attached to a metal center leads to a hydroxyl-metal specie:

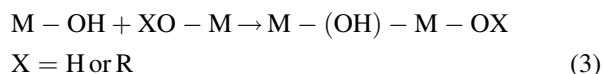


The hydroxylated metal species can react with other metal centers leading to *condensation* reactions, where

an oligomer is formed by bridging two metal centers. In the case of *oxolation*, condensation leads to an *oxo bridge*, and water or alcohol is eliminated:



In the case of *olation*, an addition reaction takes place, and a hydroxo bridge is formed. This reaction takes place when metal centers may have coordination higher than their valence, as in the case of Ti(IV), Zr(IV), or related cations,



In most sol–gel processing, the inorganic framework is built by successive hydrolysis and condensation reactions [26]. The structure, connectivity and morphology of the final inorganic network depend strongly on the relative contribution of reactions 1–3. Depending on intrinsic (i.e. metal center features such as coordination, acidity, lability...) or extrinsic (i.e. tunable reaction conditions such as solvent, water contents, pH, catalysts, reaction time...) conditions, the hydroxo-oxo-polymers thus formed can exhibit a variety of structures, from branched arrangements to compact clusters. The growth of these structures can be controlled (for example, by poisoning or by limiting aggregation), and thus *sols* made of suspended colloidal size entities are obtained. Some of these structures may grow extensively or aggregate until reaching macroscopic dimensions, trapping solvent and smaller monomers; a *gel* is thus obtained. Chemical control of activation/polymerization reactions (1)–(3) allows the tuning of the size and the shape of the inorganic polymers or colloids, as well as their miscibility (i.e. the interactions, for example hydrophobic/hydrophilic) with the organic counterparts. Functional precursors $R'-M(OR)_{n-1}$ can also be used to co-condense with $M(OR)_n$ or MX_n precursors, or to modify the surface of inorganic entities, therefore enhancing the compatibility with (bio)organic components.

2.2. Hybrid materials: classification, synthesis strategies, applications

A distinct characteristic of hybrid materials is that their properties are related not only to the chemical nature of the inorganic and organic components, but also rely heavily on their synergy. Therefore, the interface between inorganic and organic does influence strongly their properties. Hybrid materials can be thus

broadly classified in two main classes, depending on the nature of bonds and interactions existing at the hybrid interface: [9,27] *Class I* hybrids include all systems where there are no covalent or iono-covalent bonds between the organic and inorganic components. In this class, only Van der Waals, hydrogen bonding or electrostatic forces are present. On the contrary, in *Class II* hybrids, at least parts of the inorganic and organic components are linked through strong covalent or iono-covalent bonds. Hybrids can also be characterized by the type and size of the organic or the inorganic precursors. Precursors can be two separate monomers or polymers, or they can be covalently linked. Generally, phase separation between the organic and the inorganic components will occur, due to mutual insolubility. However, it is possible to obtain homogeneous or single-phased hybrids by choosing bifunctional monomers exhibiting organic and inorganic components, or by combining both types of components in phases where one of them is in large excess. The general chemical pathways used to obtain hybrid materials are schematized in Fig. 1.

2.2.1. Path A

Path A corresponds to very versatile soft chemistry based routes including conventional sol–gel chemistry, the use of specific bridged and polyfunctional precursors and hydrothermal synthesis. Via *conventional sol–gel pathways* amorphous hybrid networks are obtained through hydrolysis–condensation of various metal species (alkoxides / halides derivatives) which could be organically modified. The sol could also contain an organic component (specific organic molecule, a biocomponent or polyfunctional polymers) that can interact more or less strongly with the inorganic components leading to class I or class II hybrid materials. Alternatively, *solvothetical synthesis* has allowed the elaboration of numerous crystalline microporous hybrid solids such as zeolites and, more recently, Metal organic frameworks (MOF) [28].

2.2.2. Path B

Path B corresponds to the *assembling or the dispersion of well-defined nanobuilding blocks* (NBB) which are perfectly calibrated preformed objects that keep their integrity in the final material [10,22]. These NBB can be clusters, organically pre- or postfunctionalized nanoparticles (NP) (metallic oxides, metals, chalcogenides, etc.), nano-core shells [29] or layered compounds (clays, layered double hydroxides, lamellar phosphates, oxides or chalcogenides) able to intercalate organic components [30].

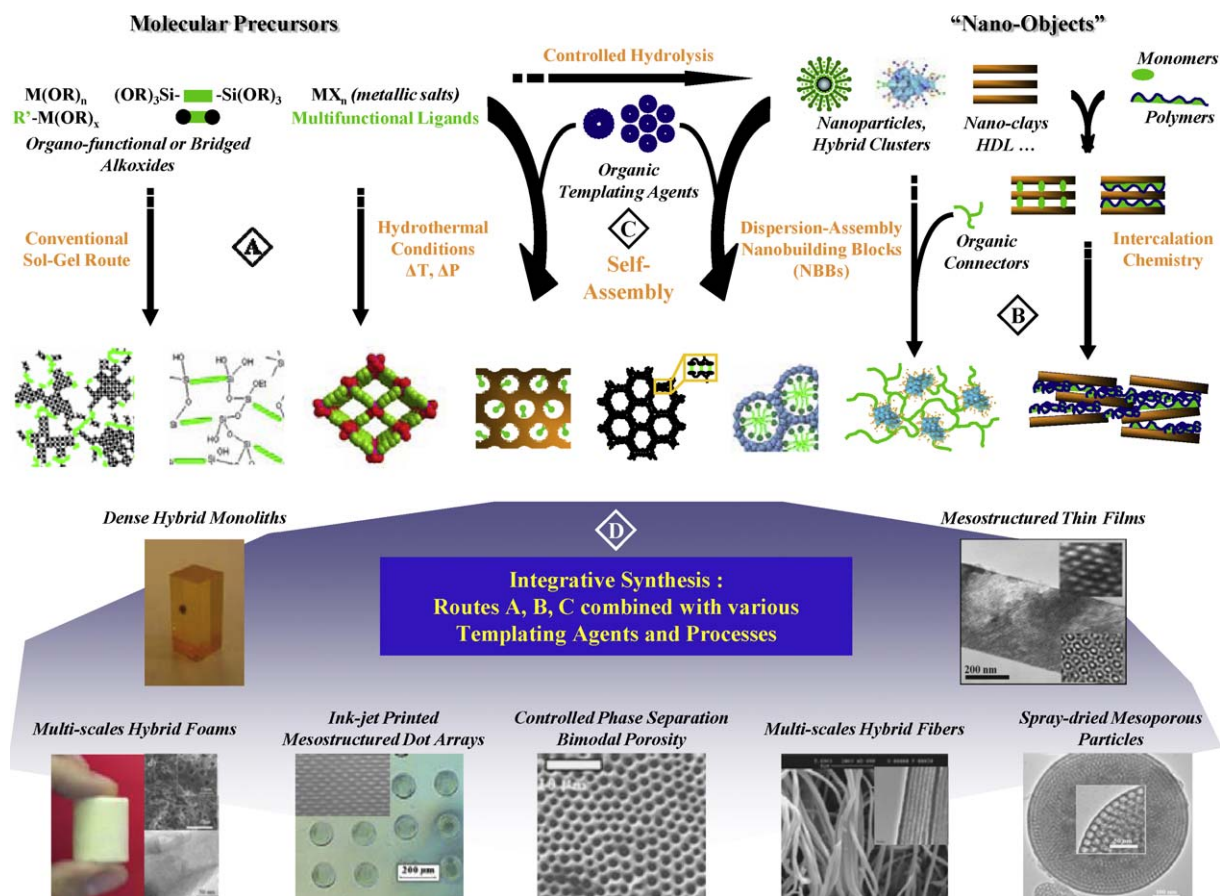


Fig. 1. Scheme of the main chemical routes leading to nanostructured inorganic and hybrid organic-inorganic materials.

2.2.3. Path C

Path C corresponds to the well-known *self-assembly procedures* which consist in the organization or the texturation of growing inorganic or hybrid networks, templated by organic surfactants [11–13,15,21,31,32]. This strategy allows a high control and tuning of the hybrid interfaces and leads to a whole continuous range of nanocomposites, from ordered dispersions of inorganic bricks in a hybrid matrix to highly controlled nanosegregation of organic polymers within inorganic matrices.

2.2.4. Path D, Integrative synthesis

The strategies reported above mainly offer the controlled design and assembling of hybrid materials in the 1 to 500 Å range. Recently, micromolding methods have been developed, in which the use of controlled phase separation phenomena, emulsion droplets, latex beads, bacterial threads, colloidal templates or organogelators leads to controlling the shapes of complex

objects at the micron scale [11,16,33–35]. The combination between these strategies and those described above along paths A, B, and C allow the construction of hierarchically organized materials in terms of structure and functions [11,12]. The chemical construction and patterning of materials with *long-range order architectures* (beyond nanometer size) remains an important challenge [2,10,12,16,36].

These versatile features, and the advancement of organometallic chemistry, and polymer and sol-gel processing, allow a high degree of control over both composition and structure (including nanostructure) of these materials, which present tunable structure–property relationships. This, in turn, allows the tailoring and the fine-tuning of properties (mechanical, optical, electronic, thermal, chemical...) in a very broad range, and the design of specific systems for applications. Hybrid materials can be processed as gels, monoliths, thin films, fibers, particles or powders. The seemingly unlimited variety, unique structure–property control,

and the compositional and shaping flexibility give these materials a high potential. Indeed, many hybrid materials have already reached a commercial status [19]. Examples include materials from electronics to automotive coatings with varied mechanical and optical properties, adhesives and composites [37]. Quite recent examples are the one million TV sets sold annually by Toshiba, [38] the screens of which are coated with hybrids made of indigo dyes embedded in a silica/zirconia matrix, organically doped sol–gel glassware sold by Spiegelau [39] and sol–gel entrapped enzymes sold by Fluka [40]. Today hybrids play an important role in the development of many functional systems as in:

- microelectronics (resistors and molding compounds, spin-on dielectrics in microelectronic interlayer, multilayer dielectric, planarization applications);
- optical systems (luminescent solar concentrators, laser dyes, sensors, photochromic, NLO or photovoltaic devices);
- micro-optics (free-standing micro-optical elements, such as a lens array on VCSEL elements for fiber coupling, diffractive lenses);
- bioactive hybrids (biosensors, bioreactors, cements in dental applications, controlled release of drugs and molecules);
- decorative and protective coatings involving scratch and abrasion resistance applications and barrier systems (solar cells, optics, electronics, food packaging...), electrochemical devices (batteries, photovoltaic and fuel cell application).

Hybrid nanocomposites based on clay-polymers are also used as effective reinforcement agents in the so-called “green” nanocomposites, with gas barrier properties and fireproof enhancements. Furthermore, these NBB based hybrids are also used in cosmetics, water-repellents, additives for paper, pressure-sensitive adhesive release coatings. Some examples of applications or systems where at least one component is based on hybrid materials are gathered in Fig. 2.

An eclectic approach to conceiving and manufacturing advanced hybrid materials necessarily includes biology, as a remarkable particularity of biological systems is their capacity to integrate molecular synthesis at very high levels of organization, structure and dynamic [1]. During the last years the field of research associated with the “biomimetic or bionspired design” of materials much increased. Industrial technologies have already been inspired by dolphin skin (Riblets in air plane wings), lily leaves (superhydrophobic coatings) and spider threads

(Nylon, Kevlar) to produce new materials [41]. However, this research field is still in its early stage of development. Bottom-up approaches based on “chimie douce” developed by Jacques Livage are opening a land of opportunities for the design of advanced functional inorganic and hybrid materials in which positioning of functionalities at different length scales are well-controlled. There is no doubt, the 21st century through a better knowledge and development of a bio-inspired integrative and green chemistry will give birth to numerous tailor made functional inorganic and hybrid materials and systems.

The subjects presented in this short background part have been extensively reviewed in their different fields, such as synthesis, properties [24,42] and applications, [19,39] textured hybrids, [11,12] and biohybrids [3,8,43]. Therefore, in the present feature article we will mainly refer to some comprehensive reviews, in order to encourage the interested reader to explore into them for more specific sources.

3. Sol derived hybrids versus NBB approaches

3.1. Introduction

Sol–gel processes, and more generally, soft chemistry routes have been used to elaborate a great variety of hybrid organic-inorganic materials, which exhibit many different interesting and useful properties [19,24]. In parallel to these routes based on molecular precursors, the NBB approach has developed with the goal of achieving hybrid materials in which the spatial extension and the architecture of the inorganic domains, as well as the nature of the interface between the organic and inorganic components, would be better defined. NBB approach is based on the assembling of well-defined and preformed objects such as metal oxoclusters (MOCs) and NPs, that keep their integrity in the final materials [10,44]. An important point in this approach is a careful control of the NBBs to provide reactive groups on their surface or anchoring sites that can react with complementary NBBs. This required functionalization can be achieved directly during the synthesis of the NBBs or in a subsequent step. Another important point is to use NBBs as well-defined as possible, i.e. with the highest possible control on their composition, size, shape, number and position of the functional groups. With this respect, NBBs based on MOCs, which are molecular species and can generally be purified by crystallization, are definitely more appealing than NPs to elaborate model systems. However, the diversity of the latter as well as the



Fig. 2. Some examples of hybrid materials applications in different fields [19].

larger sizes that can be reached makes NPs still interesting candidates to develop hybrid materials [45].

As for classical hybrid materials prepared from molecular precursors, the vast majority of the NBB derived hybrid materials are based on silicon and polyhedral oligo silsesquioxanes (POSS), many of which are now commercially available, [46] can be considered as the archetype of covalently functionalized NBBs [47]. However, NBBs based on transition metals or tin oxo-clusters are interesting because they can offer, in addition to the specific magnetic, electronic, catalytic, etc. properties associated to the metal centers, different functionalization processes that use complexing ligands or charge compensating anions [22,48,49].

3.2. Metal-oxo clusters

Transition metal oxo-clusters and especially titanium oxo-clusters offer a large variety of candidates to elaborate hybrid organic-inorganic materials by the NBBs approach. The literature describes many titanium

oxo-clusters species (polynuclear oxo-complexes), $[Ti_xO_y(OR)_z(CL)_w]$, whose size ranged from 5 to 25 Å. They exhibit a rich variety of structural types characterized by different coordination modes of the ligands (O, OR, and CL); a large diversity in linkages of the coordination polyhedra and the coordination number of titanium atoms; the degree of condensation O/Ti differs also in oxo-complexes. Their nuclearity (number of titanium atoms) reported in literature varies from two to 18 [22]. The metallic centers that exhibit coordination numbers between four and six are coordinated to bridging oxo-ligands and terminal or bridging alkoxy OR groups. A large variety of oxo bridges are encountered in the known clusters from μ_2 -O to μ_5 -O. Furthermore, numerous titanium oxo-clusters bear strongly complexing oxo-ligands CL (β -diketone, carboxylic acid, phosphonates...) with a chelating or a bridging coordination mode [22].

Among the numerous titanium oxo-clusters, we especially focused our interests on three titanium oxo-clusters, the Ti_{16} $[Ti_{16}O_{16}(OEt)_{32}]$, the Ti_8

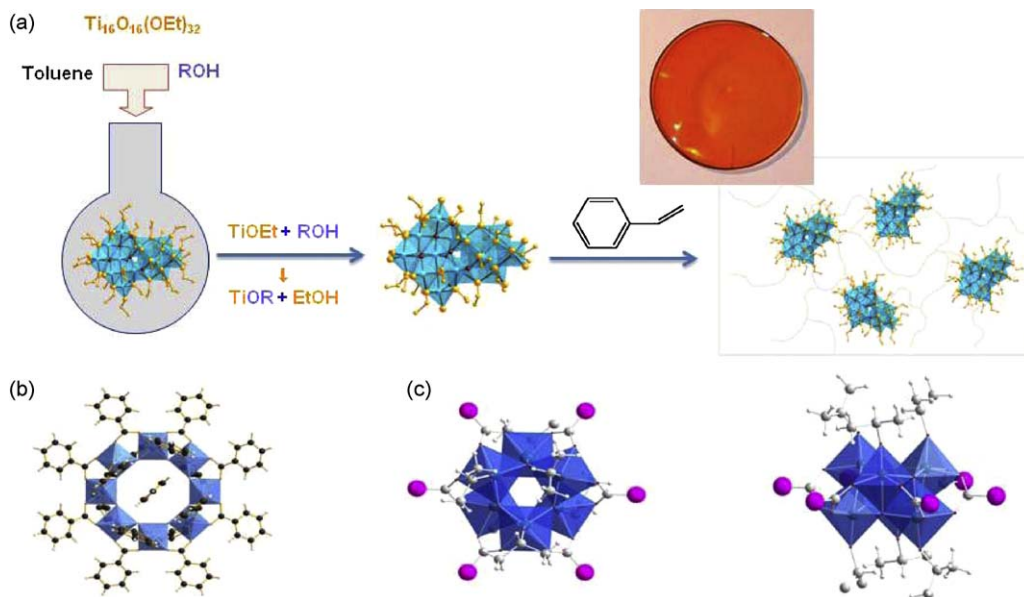


Fig. 3. a. Postmodification of the $\text{Ti}_{16}\text{O}_{16}(\text{OEt})_{32}$ cluster to form functional nano-briks and to build hybrid materials; b. Representation of the $\text{Ti}_8\text{O}_8(\text{OOCC}_6\text{H}_4)_{16}$ oxo-clusters; c. Representations of the $\text{Ti}_6\text{O}_6(\text{O}^i\text{Pr})_6(\text{OCR})_6$ oxo-clusters [22].

$[\text{Ti}_8\text{O}_8(\text{OOCR})_{16}]$, and the Ti_6 $[\text{Ti}_6\text{O}_6(\text{OR})_6(\text{OOCR}')_6]$ (Fig. 3).

The Ti_{16} oxo-alkoxo cluster, is built of an inorganic oxo-core of 16 TiO_6 octahedra, surrounded by an organic shell of 32 ethoxy groups. The specificity of this oxo-alkoxo cluster is to present labile ethoxide groups which can be selectively exchanged by transesterification or transesterification reactions while keeping the titanium oxo-core. We demonstrated the possibility to generate new titanium oxo-clusters $[\text{Ti}_{16}\text{O}_{16}(\text{OEt})_{32-x}(\text{OR}')_x]$ by postmodification of the Ti_{16} cluster [50]. Both the kinetics and the number of modified titanium atoms are strongly dependent on the nature of the new introduced ligands. The reaction between the cluster and aliphatic alcohols (such as *n*-propanol or *n*-butanol) leads to the introduction of eight new ligands on well-defined positions in the structure, even with an excess of alcohol. The use of more acidic (such as phenol derivatives), or less sterically hindered (such as methanol) reactants leads to the substitution of all the 16 terminal ethoxy by the new ligands. This behavior can be extended with the aim of forming functional titanium oxo-clusters. Based on results obtained on model reactions, NBBs with polymerizable ligands (methacrylate or styrenic), have been obtained [50]. By a judicious choice of the organic component, original architectures can also be elaborated. As an example, the assembly of well-defined dendrimers with Ti_{16} oxo-clusters has been investi-

gated and leads to nanostructured hybrid materials [51]. NMR studies allowed first the complete assignment of the 32 ligands in correlation with the crystallographic data, and in a second hand allowed to justify and quantify the formation of postmodified Ti_{16} derivatives [50,52].

The eight-membered-ring $[\text{Ti}_8\text{O}_8(\text{OOCR})_{16}]$ oxo-cluster is a very attractive NBB [53]. First, it presents no residual OR group that considerably increase its stability toward nucleophilic species. Second, the ring shape of this purely carboxylate oxo-cluster allows the building of organized hybrid edifices by the choice of carboxylate ligands.

The last presented candidate for the elaboration of hybrids by the NBBs approach, is the Ti_6 oxo-cluster $[\text{Ti}_6\text{O}_6(\text{OR})_6(\text{OOCR}')_6]$. Many times described in the literature, we can still take advantage of its particular structure. Indeed, this cluster presents at once carboxylate ligands in the equatorial position and alkoxy ligands in the axial position. Many different carboxylate ligands can be located in the six equatorial positions during the synthesis of the clusters from titanium alkoxide and carboxylic acid. In the axial position the iso-propoxide ligands on preformed Ti_6 clusters can be postmodified by transesterification reactions as demonstrated for the Ti_{16} oxo-clusters. The simultaneous presence of carboxylate located perpendicularly to the alkoxy ligands allows the building of directional hybrid edifices.

3.3. Nanoparticles

Though less well-defined, nanoparticles (NPs) represent a rich and versatile alternative to metallic oxo-clusters in the NBB approach to hybrid organic-inorganic materials. Many compositions, crystalline structures and shapes can be obtained with size ranging from few nanometers to few tenths of microns. As for clusters, a crucial point remains a careful control of their functionalization, [45] which is generally necessary to stabilize, to give new properties and to make them compatible with the application medium.

As mentioned in the general background (part 2), the sol-gel process can be conveniently used to prepare a stable suspension of metal oxide NPs. One way is to control the growth of the oxo-framework through a poisoning process with complexing ligands that, at the end, remain on the surface of the particle and provide a way to functionalize them [54]. Such an approach was used with a pyrrole functionalized β -diketone as complexing ligand and TiO_2 anatase NPs with pyrrole groups grafted on the surface were produced from titanium alkoxides in a one step process [55]. The dangling pyrrole groups were subsequently chemically or electrochemically polymerized, and films made of TiO_2 anatase NPs (2–4 nm) homogeneously distributed in a matrix of short polypyrrole chains were prepared on ITO coated glass. The cyclic voltametric response of these films was stable and reversible.

Another family of NPs that has attracted attention in the last few years is the so-called “Janus-head” type NPs, which exhibit a dissymmetric distribution of two functions at their surface and are accordingly named from the two faced Roman god [56]. These objects are especially interesting for their potential properties in the field of self-organization. However, their elaboration usually requires a multistep process that involves reaction at an interface or the fusion of two different hemi-objects. Moreover, the stability of the dissymmetry relies on a strong and irreversible anchoring of the functions on the surface of the final object in order to prevent any relaxation towards a homogeneous distribution. Recently, thermodynamic Janus NPs were prepared in one step from gold cores functionalized with two ligands: a diphenylphosphinine, 3,5-(C_6H_5)₂($\text{C}_5\text{H}_3\text{P}$), and a thiol (RSH) [57]. The quite different physicochemical properties of these two ligands cause their phase separation on the surface of the NPs and create a dissymmetric distribution of the capping molecule. Moreover, the different electron donating-electron withdrawing abilities of these ligands, in association with their dissymmetric distribution, cause a blue shift of the localized

surface-plasmon band, with respect to the gold NPs capped by only one of the two ligands. Finally, when an hydrophilic thiol was used ($\text{HS}-(\text{CH}_2)_{10}-\text{CO}_2\text{H}$), self-organization behavior was also evidenced.

3.4. Mechanical and optical properties of the resulting hybrids

The introduction of fillers in polymer matrices meets a well-established industrial scheme that aims at enhancing specific properties of polymers while reducing production costs. The regularity of the dispersion of the organic and inorganic phases and the extended and controlled interfaces between the two phases encountered in hybrid materials offer the possibility to control the mechanical properties. High performance in term of mechanical responses has been reported for hybrids based on calibrated nano-objects (MOCs and NPs) which allow the control of the degree of organization and the size and the nature of the hybrid interfaces [20].

Functionalized titanium oxo-clusters ($\text{Ti}_{16}\text{O}_{16}(\text{OEt})_{32-x}(\text{OR})_x$, x = metacrylate or styrenic groups) were copolymerized with organic monomers (metacrylate or styrene) to obtain organic-inorganic hybrid networks. The postmodification of the NBBs allows limiting phase segregation between both components; hybrid networks are formed in which the oxo-clusters are covalently linked to the organic matrices. These oxo-clusters play the role of nano-sized cross-linkers, well dispersed in the host media. A significant reinforcement of polymers has been observed, especially in the rubbery regime (Fig. 4) [58].

Coatings with efficient mechanical properties, investigated by the nanoindentation technique, have been elaborated by introducing goethite (α - FeOOH) nanorods or maghemite (γ - Fe_2O_3) nanospheres in a poly(hydroxyethyl methacrylate) (PHEMA) matrix. Both goethite nanorods and maghemite nanospheres yield a strong reinforcement effect of PHEMA, even at low volume fraction. The origin of such reinforcement is attributed to the existence of strong interactions at the iron oxide-PHEMA interface combined with a homogeneous dispersion of the particles. The chemical modifications of the organic component by the iron oxide particles (hydrolysis of the ester yields carboxylate which complexes iron sites) favor the high mechanical performance of the resulting hybrids (Fig. 4). By the control of the specific interactions between the particles and the polymer matrix, the particles are likely to be used as functional reinforcing elements. Nanocomposites are then synthesized in

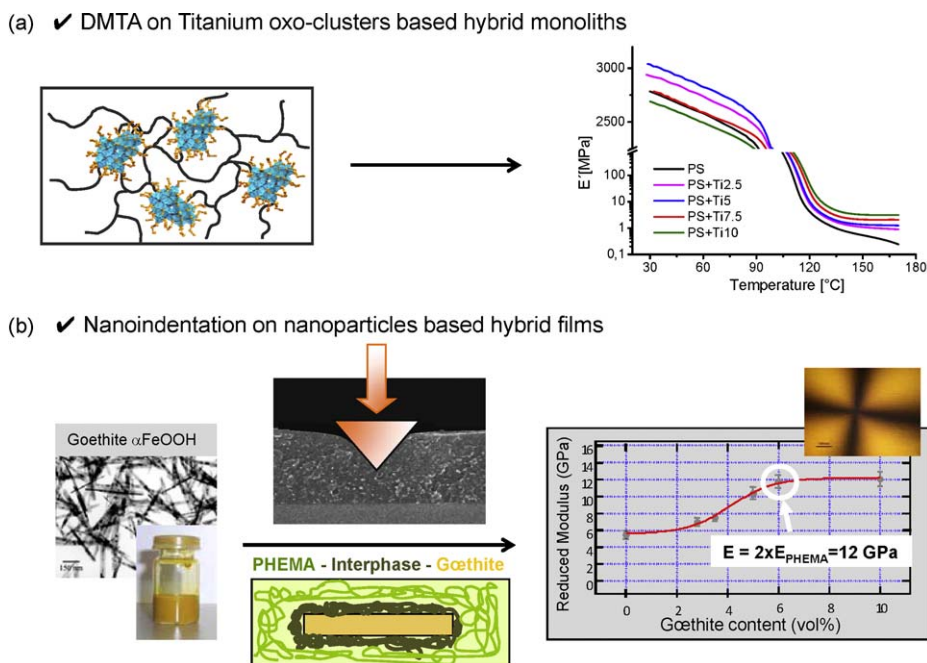


Fig. 4. a. Reinforcement of polymers by covalently bonded nano-crosslinkers [58]. b. Mechanical properties by nanoindentation of functional hybrid coatings based on anisotropic iron oxide nanoparticles dispersed in poly(hydroxyethyl methacrylate) [45].

which the polymer acts as binder that fixes the functional nanoparticles while the particles bring the functionality of the hybrid material and participate to the mechanical reinforcement [45].

Nowadays, abundant optical devices, luminescent solar concentrators, dye laser, sensors, photochromic, NLO and photovoltaic devices, based on sol-gel derived hybrid materials have been referenced [18,59]. Most of the optical properties are brought by the incorporation of organic molecules into inorganic oxide matrices [18]. The optical behavior of hybrids can also evolve from the inorganic component of the hybrids. We recently reported hybrid coatings based on goethite iron oxide nanoparticles (cf. mechanical properties of hybrids). In addition to the coloration of the samples, due to the presence of the nanoparticles, the coatings exhibit interesting birefringent properties associated to the stabilization inside a polymeric organic matrix, the poly(hydroxyethyl methacrylate) PHEMA, of a liquid crystal type organization resulting from the self-organization of the highly anisotropic goethite nanorods (Fig. 4). Concentrated and stable aqueous dispersion of goethite particles behave as nematic lyotropic liquid crystals with interesting magnetic properties. The same behaviour is also encountered in a glassy polymeric medium [45].

The incorporation of titanium oxo-clusters as additive into already known ORMOCER[®] matrix materials offers a variety of new hybrid materials for high added-value applications, for example in micro-optical devices. The refractive index and the optical loss measurements, key parameters for micro-optical applications, of the resulting materials have been recently investigated [60]. The refractive index of a material, in close relation to its permittivity, depends on the polarizability of a substance. The use of a titanium oxo-cluster, $[\text{Ti}_6\text{O}_4(\text{OCC}_6\text{H}_5)_8(\text{O}^i\text{Pr})_8]$, which bears both aromatic groups and titanium, a transition metal with high polarizability, results in a significant increase of the refractive index. Moreover, the nanometer size of the titanium oxo-clusters limit the scattering of the resulting nanocomposites, and the very high optical qualities of the ORMOCER[®], used for optical waveguides, is not affected.

NBBs based hybrids are also useful models to understand the optical behavior of conventional nanocomposites. Thus, the $[\text{Ti}_{16}\text{O}_{16}(\text{OEt})_{32}]$ oxo-clusters based hybrid materials were used as a reference sample to compare its photosensitivity with that of TiO_2 gel-based hybrid materials. Less attention is paid to the photochromic properties of TiO_2 based materials. Nevertheless, it is well known that the reduction of Ti^{4+} into Ti^{3+} undergoes strong darkening of TiO_2 based

samples. However, in most cases spontaneous reoxidation occurs, leading to the concomitant discoloration of the samples. The oxidation of the Ti^{3+} sites can be restricted and the coloration stabilized by the elaboration of TiO_2 based hybrids, in which the inorganic photoactive component is generated simultaneously with a polymeric component [61]. We showed that the electronic coupling along the extended interface between the inorganic, and the organic, poly(hydroxyethyl methacrylate), interpenetrated networks allows:

- a rapid scavenging of the photo-excited holes by the polymer;
- an efficient trapping of the photo-excited electrons as small polarons (Ti^{3+}) that develop “dark” absorption continuum covering the spectral range from 350 nm (UV) to 2.5 μm (IR);
- their long-term conservation over months at high number density (Fig. 5) [61,62].

Furthermore, we observed that the electron transfer depends on the material microstructure, which can be affected by the materials chemistry and processing. Undeniably, tuning the delay between the gelation of the system and the organic polymerization step, or using NBBs as an inorganic reference species allows the optimisation of the photochromic responses of the resulting nanocomposites [62].

4. In situ evaluation of hybrid interfaces and their evolution

4.1. Affinity by DOSY NMR in the colloidal state

The chemical syntheses of nanoparticles (NPs), through a bottom-up approach, very often use organic

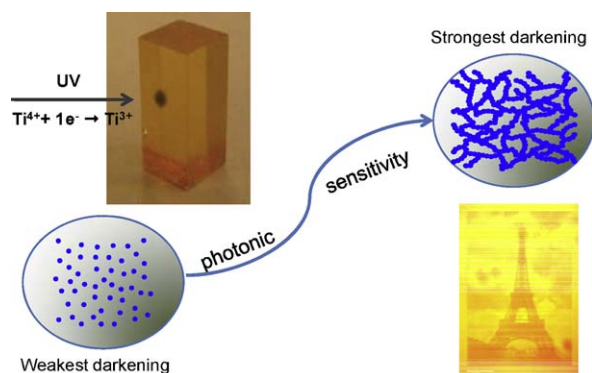


Fig. 5. Laser-induced photopatterning of organic–inorganic TiO_2 -based hybrid materials with tunable interfacial electron transfer [61,62].

capping agents to control the size, the size-dispersity, the morphology, the crystalline structure, and the stability. Such syntheses yield suspensions in which the NPs are protected by a shell of capping molecules that, in addition to the role played during the synthesis, can also modulate the properties of the NPs. The use of NPs also often relies on the functionalization of their surface. This step can be required to make them compatible with the application medium or to create new functionalities at their surface (sites with specific molecular recognition properties, unsaturated groups that can polymerize, etc.). Indeed, many NPs based suspensions can be considered as true hybrid organic-inorganic systems. A fine characterization of the surface chemistry of NPs is therefore highly necessary to understand and improve the synthesis and to rationalize the utilization of NPs. In particular, measuring the affinity of organic molecules for NPs, in suspension, is of prime importance. However, evaluating this affinity in situ is not a simple task, especially when the capping molecules are involved in a dynamic equilibrium between a free form and a grafted form (Fig. 6).

In such a context, Diffusion Ordered Spectroscopy (DOSY) NMR has been evidenced as an efficient tool. This technique, which belongs to pulsed field gradient methods, provides in addition to the classical data of solution NMR, i.e. chemical shifts and scalar coupling constants, a way to measure self-diffusion coefficients, which can be used to sort species according to their size, as the diffusion coefficient is inversely proportional to the hydrodynamic radius [64]. Accordingly, free molecules can be differentiated from those that interact with NPs as their diffusion coefficients are different. Moreover, a careful exploitation of the data allows one to quantify the populations associated to the different self-diffusion coefficients [65]. This technique combines the well-known high selectivity of NMR, able to spectroscopically differentiate many components in a complex mixture, with the absence of any physical separation step.

The first uses of DOSY NMR in the context of inorganic NPs were on monolayer-protected gold clusters (MPCs). In these studies, DOSY NMR was only used to measure the hydrodynamic size of the MPCs [66]. In 2005, the first use of DOSY NMR to prove the functionalization of NPs was reported [67]. This study was performed on nano- CeO_2 functionalized by carboxylic acid, and while standard 1H NMR gave no information on functionalization, grafted and free ligands were clearly differentiated and quantified using DOSY NMR experiments. The same year, the use of DOSY NMR to assign the 1H resonances of

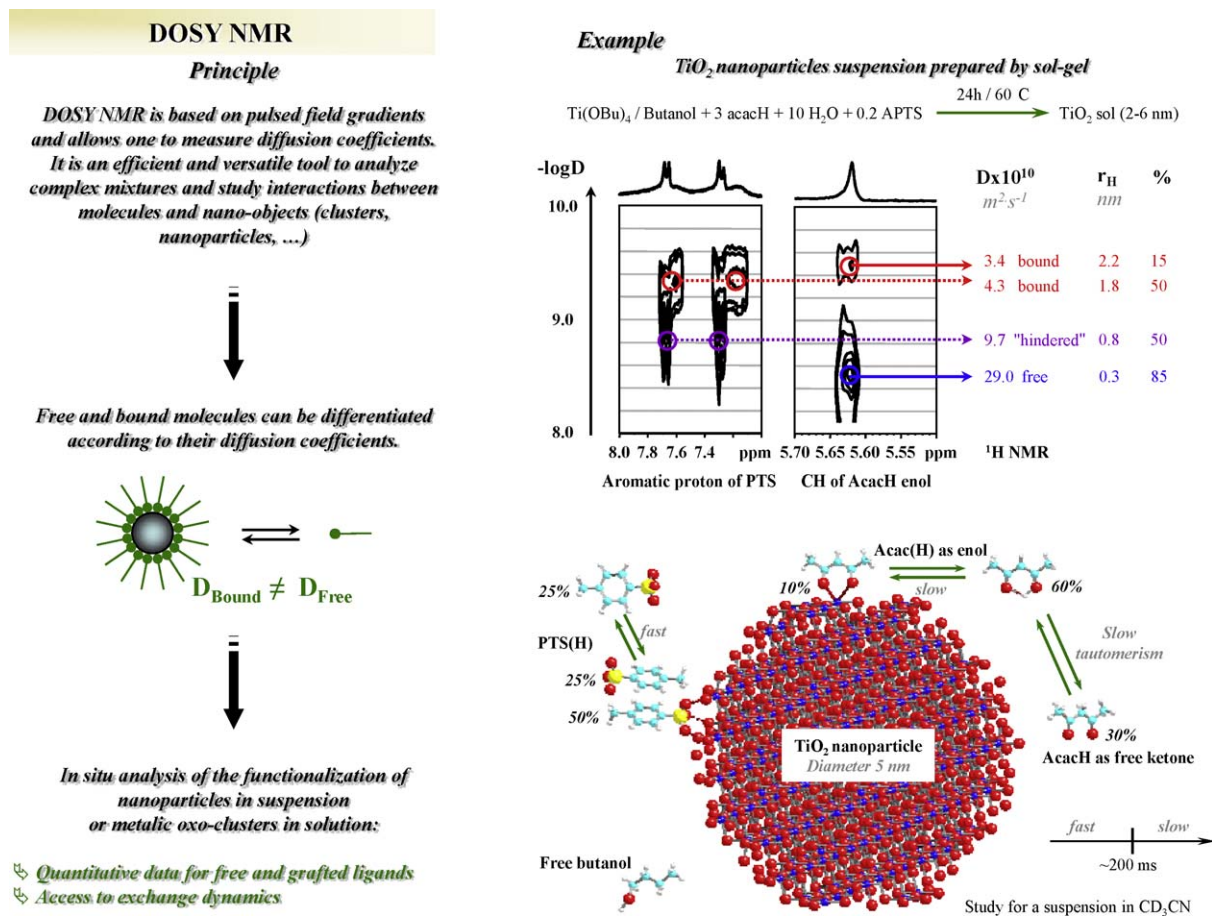


Fig. 6. Diffusion Ordered Spectroscopy (DOSY) NMR can be used to analyzed in situ the functionalization of nano-objects, such as NPS or MOCs. The example on TiO₂ nanoparticles is taken from reference [63].

TOPO molecules interacting with InP quantum dots (QDs) was also reported [68]. In this system (TOPO@InP in toluene), free and bound TOPO molecules exhibit different ¹H chemical shifts and, therefore, can be quantified “classically” by integration in the spectroscopic dimension. In 2006, this quantification method was used to report the adsorption isotherm of TOPO on 4.7 nm InP QDs at 295K [69]. The free energy (ΔG^0) for the adsorption was measured and a Fowler isotherm was shown to better describe the adsorption than a simple Langmuir isotherm, pointing out the non-negligible and favorable role of TOPO–TOPO interactions in the process. In 2007, a complex multicomponent sol–gel derived-system containing TiO₂ NPs (2–6 nm), acetylacetone (acac), *p*-toluenesulfonic acid (pTs), and butanol was investigated (Fig. 6) [63]. DOSY NMR clearly showed that:

- the enol form of acac was present as grafted and free species while its diketone form was found only as free molecules;
- pTs was distributed between strongly interacting molecules, weakly interacting molecules and free ones, the two last types being in rapid equilibrium;
- butanol was not interacting with the NPs. All these species were also quantified. More recently, other reports on the use of DOSY NMR for NPs have been published [70].

When the lifetimes of species involved in a equilibrium ranges from ca. 10 ms to ca. 1 s, information on the dynamic of the systems can be extracted from DOSY NMR [71]. Recently, we have used this approach for TOPO molecules adsorbed on CdSe QDs and we have been able to estimate the lifetime of the bound species to ca 0.6 s [72]. In conclusion, for favorable cases, not only

thermodynamics data can be evaluated but information on the dynamic can also be obtained.

In the context of hybrid materials built from well-defined metallic oxo-clusters, [10,22] DOSY NMR is also a valuable tool to study the functionalization of these molecular NBB. In the case of the macro-cation $\{(R\text{Sn})_{12}\text{O}_{14}(\text{OH})_6\}^{2+}$, which can be functionalized and/or assembled through its charge compensating anions, [48,73] DOSY NMR was used to study the influence of the solvent on the ionic dissociation and anion exchange [74].

4.2. Self assembly: Interface class

I – SAXS / Ellipsometry

As mentioned previously, one of the major issues leading to a high control of the final nanomaterials lies in the characterization of the hybrid interfaces all along the formation mechanisms. However, in the case of mesostructured thin films coated onto a substrate or meso-organized particles prepared by spray-drying, the very small amount of matter (usually for thin films [15] between 10 and 500 $\mu\text{g}/\text{cm}^2$ and for particles 6 $\mu\text{g}/\text{cm}^3$ in the gas phase [75]) requires very sensitive techniques for their whole characterization. In this way, synchrotron 2D-SAXS techniques, used for the structural characterization of mesophases, are very efficient for three main reasons. This technique is not limited by the low amount of matter and then could be applied for the analysis of mesostructured materials shaped as (ultra) thin films [15,76,77] and particles [75] generated by spray-drying. It also leads to a straightforward and non-ambiguous characterization of the structural periodic organization of the mesoporous network on the contrary to the conventional (1D) laboratory XRD techniques. Moreover, the high X-ray flux provided by synchrotron sources allows in situ time-resolved SAXS experiments which are of great importance for a deep understanding of self-assembly mechanisms and (rapid) mesophase transformation specially when coupled with other techniques as interferometry, WAXS or ellipsometry.

For example, we studied the structural evolution of meso-organized thin films just after coating by in situ time-resolved SAXS experiments coupled with interferometry [78,79]. By recording 2D-SAXS diagrams every 20 seconds or 5 minutes (depending on the system studied), we investigated independently the influence of the chemical parameters (e.g. pH, aging time of the solution, initial sol composition...) and processing conditions (e.g. partial vapor pressures, temperature...) on the self-assembly mechanisms [76,77]. These specially designed experiments allowed

us to improve the synthesis of silica-based mesostructured materials (in particular the influence of various organosilica compounds on the final mesostructure) and to explore the field of non-silicate, transition metal oxide, rare earth oxide and multi-metallic based mesostructured materials (ZrO_2 , [80] TiO_2 , [81,82] V_2O_5 , [83] $\text{ZrO}_2\text{-CeO}_2$, [84,85] $\text{ZrO}_2\text{-Y}_2\text{O}_3$, [84] $\text{TiO}_2\text{-Nb}_2\text{O}_5$, [86] HfO_2 , [87] WO_3 , [88] SnO_2 , [89]...).

These latter materials could be designed with amorphous or nanocrystalline walls opening new opportunities for the development of many applications arising from the active properties (optic, electronic, magnetic...) due to the presence of metallic centers having *d* or *f* orbitals. However, the crystallization process is not straightforward [15,76]. The crystallization of the inorganic walls often leads to a collapse of the mesostructure due to nucleation-growth mechanisms. Then the experimental conditions (maximum temperatures, time of the treatment, heating rates, sequential steps, storage conditions, nature of block copolymers...) are critical in order to promote crystallization while avoiding mesostructure collapse. The optimal experimental conditions, for a given system, were determined precisely via in situ SAXS-WAXS experiments [82,90,91]. Briefly we analyzed simultaneously during the thermal treatment the evolution of the mesostructure by in situ SAXS and the crystallinity of the network composed of crystalline NPs by in situ WAXS (Fig. 7). It was then possible to synthesize new crystalline mesostructured thin films such as SrTiO_3 perovskite, [90] tetragonal MgTa_2O_6 , [90] $\text{MTiO}_3\text{-TiO}_2$ ($\text{M} = \text{Co}^{\text{II}}$ or Ni^{II}) (ilmenite – anatase/rutile), [90,91] $\gamma\text{-Al}_2\text{O}_3$, [92] cubic Eu_2O_3 , [93] cubic Y_2O_3 , [94] Nb_2O_5 [86], etc.

In order to fully understand crystallization mechanisms, the in situ SAXS-WAXS experiments were recently completed by in situ thermal ellipsometric analysis [95]. This lab-scale technique, more accessible than synchrotron experiments, gives access to the index of refraction and film thickness during heating. These informations were used to evaluate the evolution of the porosity and material composition as a function of temperature, thus identifying key parameters that affect densification, pyrolysis, crystallization, and sintering (an example is shown in part 5). The influence of the heating schedule, the initial film thickness, the nature of the substrate, the solution aging, the presence of water during calcination, the nature of the templating agent, and the influence of additives (H_2O , HCl) in the calcination environment were studied on the index refraction profiles as a function of temperature. These

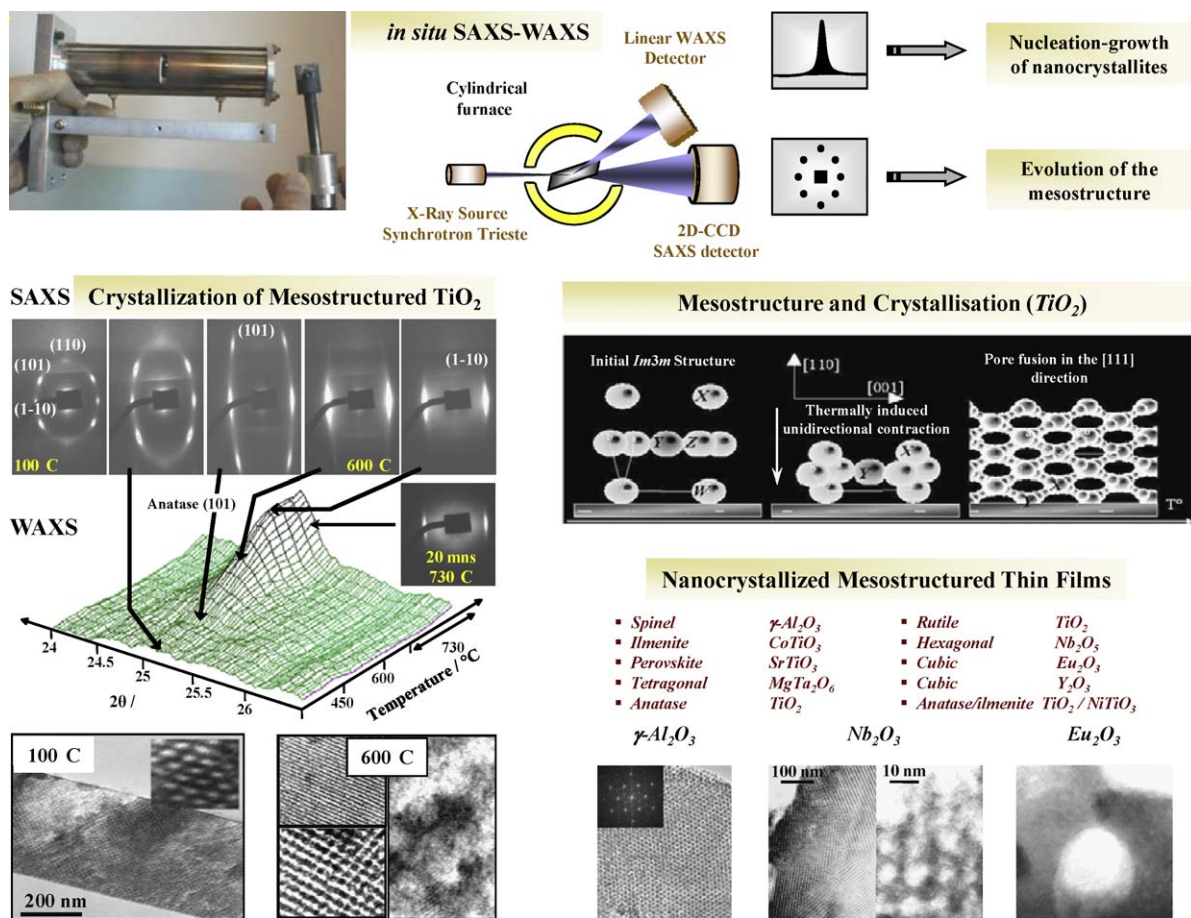


Fig. 7. Top: Experimental scheme of the SAXS-WAXS experiment. Left: SAXS-WAXS patterns of mesostructured TiO_2 thin films during thermal treatment. Right: Transformation of the initial $Im\bar{3}m$ mesostructure into a “grid-like” nanocrystalline structure [82,90,91]. Examples of different nanocrystalline mesostructured thin films [86,92,93].

parameters are shown to have unique and often substantial effects on the final film structure.

5. Nanoporous materials

5.1. Periodically Organized Mesoporous Thin Films (POMTFs) by EISA

Up to now, the preferential way of POMTFs synthesis is the EISA approach (for more detailed information about POMTFs, we recommend the following reviews [15,21,76,77,96,97]). Briefly, the EISA process (Fig. 8) implies first the elaboration of an isotropic dilute solution containing mainly inorganic (or hybrid) precursors, solvents, catalysts and molecular templating agents.

In a second step during coating processing, the fast evaporation of volatile species (typically ethanol, THF,

HCl, H_2O) triggers the self-assembly process by concentrating progressively the system in inorganic precursors and surfactant. In due time, the concentration in surfactant reaches the equivalent of a critical micellar concentration for the system, and then micelles start to form, surrounded by the inorganic precursors. An alternative way has been recently published implying block copolymers PS-*b*-PEO of high molecular weight which exist in the micellar state in the starting solution. This process was called Evaporation Induced Micellar Packing (EIMP). EIMP is particularly useful to create mesoporous layer with difficult systems (RuO_2 and multicationic oxides) [90,100]. Depending on the processing conditions (i.e. water and solvent relative pressures, temperature), the micelles could self-organize on a large scale leading to a liquid-crystalline phase before the extended condensation of inorganic species will lock the system. This step is addressed as the

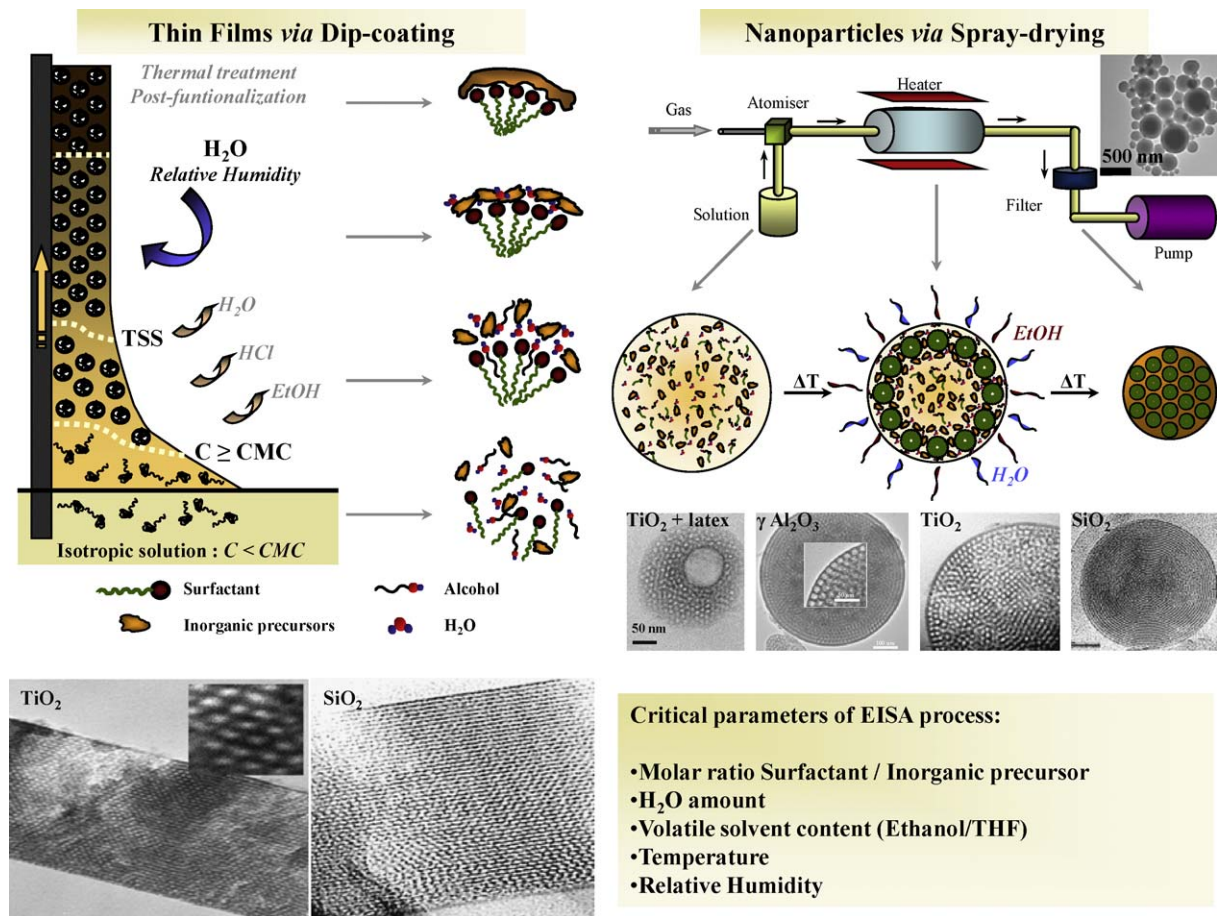


Fig. 8. Schematic representation of EISA mechanism via dip-coating and spray-drying processes [15,75,77,79,98,99].

Tunable Steady State (TSS). The third step is dedicated to the removal of the surfactant, the stiffening of the inorganic network and eventually the crystallization of the inorganic walls. The EISA approach is not straightforward since it implies competitive processes: inorganic condensation versus organic meso-organization, both of them being influenced by the diffusion of the volatile species. In the following paragraphs, we will emphasize some critical aspects of the synthesis of nanocrystalline mesostructured thin films and hybrid thin films synthesized via EISA approach.

5.1.1. The initial solution

The prerequisites concerning the initial solution are numerous. This latter has first to be highly homogeneous and stable with time. Self-assembly requires mobile and flexible inorganic species able to accommodate to the curved surface of micelles and to interact with the hydrophilic part of the surfactant. pH, aging time, water content, solvent and to a lesser extent

dilution (crucial parameters in sol-gel chemistry) have to be carefully controlled in order to generate hydrolyzed but slightly condensed inorganic species in the starting sol. These prerequisites could be difficult to manage with the synthesis of (multi)metallic oxides-based or hybrid silica-based POMTFs. Despite the well-established conditions for pure silica and titania [77], the situation becomes much more complicated with multimetallic oxides and organosilanes species.

For metal oxides, experimental conditions have to be selected with respect to the speciation diagram of cations in aqueous solution. Generally, with trivalent to pentavalent cations (e.g. TiO_2 , ZrO_2 , Al_2O_3 , Nb_2O_5 , ...), high hydrochloric acid content in the solution is required to inhibit an extended condensation of the inorganic species. The difficulty arises for the synthesis of multimetallic oxides-based POMTFs (perovskite $SrTiO_3$, tetragonal $MgTa_2O_6$, ilmenite $MTiO_3$ ($M = Co^{II}$ or Ni^{II})) since these compounds correspond to solid solutions. It is then necessary to

adjust the solution conditions to solubilize conveniently all the species (a wise choice of the metallic precursors, salt or alkoxides, must be done) and to avoid condensed species which could favor nanocrystalline phase segregation in the final material [90]. However, it could happen that ideal solution conditions, suitable for all the cations, do not exist reducing then considerably the time window of solution coating.

Difference of reactivity and solubilization difficulties are also encountered with hybrid silica-based mesostructured materials synthesized by a “one-pot” procedure [15,96,101]. With hydrophobic species, hardly soluble in ethanol, the replacement of a part of ethanol by THF is the solution widespread due to both its high solubilization abilities and physicochemical properties close to those of ethanol [15,102]. It is also important to point out that the amount of cosolvent in the initial sol should be adapted to avoid phase separation during the evaporation step (higher than the quantity necessary to solubilize the organosilane especially when its boiling point is lower than that of ethanol). The presence of organosilanes could also modify the hydrolysis-condensation kinetics of silica species modifying then the self-assembly process or even hindering mesostructuration [103,104].

5.1.2. Self-assembly induced by evaporation

The self-assembly constitutes also an intricate stage leading to the formation of a hybrid mesophase composed of an ordered micellar arrangement embedded within a stable amorphous inorganic medium. Indeed, it can be divided in four main steps, kinetically (steps 1 and 4) or thermodynamically (steps 2 and 3) governed, which could overlap all along the coating process: (1) fast evaporation of solvent(s), (2) equilibrium of atmospheric water (relative humidity) with water inside thin film, (3) formation and stabilization of the hybrid mesophase and (4) stiffening of the network by extended condensation.

Solvent evaporation and water equilibrium (steps 1 and 2) must be as fast as possible. Indeed the aim is to limit as far as possible chemical modifications and possible phase separation resulting from solubility heterogeneity between non volatile species (i.e. cations or hydrophobic organosilanes aggregation). Moreover, since water molecules inside thin films play an important role (micellar curvature and viscosity variations, hydrolysis of the remaining non-hydrolyzed precursor) in the formation of the liquid-crystalline phase, the fast water equilibrium appears to be a critical point due to the competition of this process with the inorganic condensation. The third step is the Tunable

Steady State where the system is flexible enough for further modifications (slight condensation of inorganic species) and where its composition is in equilibrium with the environment. At this stage, changes in the atmosphere composition (i.e. relative humidity) could lead to modifications of the mesostructure. For example, it is usually observed that a high relative humidity within the deposition chamber favors mesophases with high micellar curvature (cubic structure) for low surfactant content. This general tendency could be somehow modified by the incorporation of functional organosilanes in the starting sol (“one-pot” synthesis). Depending on the nature of the functional group (hydrophobic, hydrophilic, ionic, aromatic, polar, apolar) and the length of the organic chain between the functionality and the anchoring group ($-\text{Si}(\text{OR})_3$), various modifications of the mesostructure could be observed from simple variations of the lattice parameters [103] to phase transitions, [102,105] and even the formation of a mesophase for a (very) low molar ratio of surfactant/silica which leads usually to amorphous thin films without organosilanes [106]. Since TSS is a relatively slow stage for metal oxides (it can last a few hours while it takes few seconds with silica-based systems due to different condensation rates of inorganic precursors), the mesostructure is retained by aging thin films in a humidity-controlled atmosphere before a prethermal treatment step. Indeed, it has been shown that a long prethermal treatment below the crystallization temperature is beneficial since the inorganic network slowly condenses by dehydration and full departure of the remaining condensation inhibitor, HCl. For multimetallic oxides, this humidity-controlled aging step must be limited sometimes, in order to prevent demixing and aggregated clusters formation due to the differences in solubility and condensation kinetics of metallic centers [90]. The use of surfactants presenting a high hydrophobic-hydrophilic contrast such as KLE, PS-*b*-PEO, PIB-*b*-PEO block copolymers, which favor fast micellization and mesostructuration, is then required. In this case, the slight thermal treatment applied just after TSS is preferred.

5.1.3. The thermal treatment

The aim of this step is to consolidate the inorganic network, to remove the templating agent (once the inorganic walls are sufficiently rigid to prevent collapsing of the mesostructure) and eventually to promote crystallization of the inorganic walls. It has to be modulated following the nature of thin films. With hybrid mesostructured thin films, temperature and

duration of the thermal treatment have to be adapted: stiffening the inorganic network without decomposing functional organosilanes. The thermal treatment is usually followed by a washing step, which allows the extraction of surfactant [102,105]. For metallic oxides, the processes involved are more complicated especially when crystallization of inorganic walls is the aim. As it was mentioned previously, a prethermal treatment at low temperature is usually applied after TSS. It prevents a too high deformation of the mesostructure upon removal of the organic phase and further crystallization. This prethermal treatment is then followed by the decomposition of the template at higher temperatures. The third step of thermal treatment is about the crystallization process. One must keep in mind that crystallization occurs through nucleation and growth of crystallized seeds and is followed by diffusive sintering if a sufficiently high temperature is maintained long enough. To retain a highly organized mesostructure, generally a fast homogeneous nucleation must be favored at the same time that an extensive diffuse sintering must be avoided. It was also observed that the presence of a high surface area associated to thin inorganic walls tends to delay crystallization and stabilize metastable phases. Moreover, the role of the surfactant during the crystallization process is of great importance since mesostructure collapsing is observed when the thermal decomposition of surfactant occurs before dehydration process is completed (as in the case of Al_2O_3) [107,108]. KLE or PS-*b*-PEO surfactants are then preferred to pluronic block copolymers since their hydrophobic part (polyethylenecobutylene or polystyrene) decomposes at higher temperature than the hydrophobic polypropylene part of pluronic templates.

Although a deep knowledge of formation mechanisms is a first requirement for designing well-adapted materials for a given application, many applications require a real assessment of the textural characteristics of materials (i.e. surface area, porous volume, pore size distribution, pore connectivity, diffusion phenomena). For powders, such investigations are usually done via gas adsorption/desorption experiments. However, the small amount of matter and the presence of substrate limit considerably such analyses. Among textural techniques dedicated to thin films (Surface Acoustic Waves [109], krypton physisorption [110], X-Ray Reflectivity porosimetry [111]) spectroscopic ellipsometry porosimetry [112,113] is widely used. Two possible setups are nowadays accessible. The first one (ellipsometric porosimetry) consists of a spectroscopic ellipsometer on which a vacuum chamber is fixed. A known and progressive quantity of absorbate is introduced into the

chamber and the optical density value is recorded once the absorbate pressure is stabilized [112,114]. The second one (environmental ellipsometric porosimetry) works under atmospheric conditions where a continuous flux of air containing a controlled relative pressure of gas (usually water or alcohol) is applied at the sample surface [113]. This last setup allows a shorter analysis time (1 h for a complete adsorption–desorption isotherm instead of around 8 h with sealed chamber) and is very advantageous for the simulation of environmental adsorption of gas. EP and EEP offer the opportunity to determine not only classical textural properties but also the thickness of thin films during absorption–desorption of gas and then their mechanical properties (transverse Young's modulus E). EEP was successfully used to investigate the stability of mesostructured thin films. It was, for example, observed that pure silica meso-organized thin films were poorly stable in simulated body fluid on the contrary to Zr (or Al)-loaded SiO_2 mesoporous thin films, TiO_2 films being the more stable [115]. The stability of mesostructured thin films is not only environmental conditions dependent but is also function of the mesostructure's geometry. For SiO_2 POMTFs, the most often obtained and reported 2D-hexagonal structure collapses in the presence of water, while tridimensional phases (cubic and 3D-hexagonal ones) exhibit longer lifetimes [116].

5.2. Properties of mesoporous thin films by EISA

This part concerns the properties of periodically organized mesoporous architectures including thin films and membranes. These materials exhibit unexpected electrochemical, catalysis and photocatalysis properties because the mesoporous network serves as efficient pathways for molecular transport or/and the connected solid network allow fast transport of electrons, oxygen ions, protons throughout the nanoarchitecture. Because these nanoarchitectures exhibit high surface-to-volume ratios, they also serve as tools to amplify the critical phase of any electrochemical system: the interface. The sol–gel based chemistry and the processing involved for their synthesis allow a facile control of the solid and pore network with tuned properties. We will describe in this paragraph the recent research on mesoporous thin films as new materials in photocatalysis, photovoltaic, electrochemical/sensing and, fuel cell applications.

5.2.1. Photocatalyst

The continuous organized mesoporous network on TiO_2 mesoporous thin films facilitates the flux of

reactant molecules that access the catalytically active “internal surface” area. The efficiency of photon–energy conversion in these systems has been shown to readily depend on the pore-size and its distribution [117]. For example, in TiO_2 mesoporous thin films, efficient photocatalytic properties are reached for mesoporous films exhibiting a cubic mesophase with pores of 7.5 and 5.5 nm, respectively. In these studies, the modification of the film porosity with the heat treatment was followed by Ellipsometry Porosimetry. The corresponding isotherm shows the opening of the structure and the stabilization of the porous network between 500 and 600 °C. The highest decomposition rate of methylene blue (MB) is obtained for mesoporous TiO_2 films heat-treated at 600 °C (Fig. 9 left part). Additionally, the crystallinity and the structure of the

inorganic network forming the pore wall influence the photon-energy conversion. In TiO_2 mesoporous film, high crystallinity with an open grid-like mesophase structure seems to be the best conditions for efficient photoactivity.

The efficiency of photon-energy conversion can be increased by using visible wavelength photons. Their captation is promoted by doping the TiO_x ($x < 2$) structure with nitrogen centres, the presence of which decreases the anatase band-gap [118]. The decomposition of lauric acid coated on mesoporous N-doped titania films is highly efficient for films nitrated at 500 °C. These mesoporous films contain an optimal surface concentration of nitrogen since the oxygen vacancies are still not important enough to promote the recombination of the photogenerated electrons and holes.

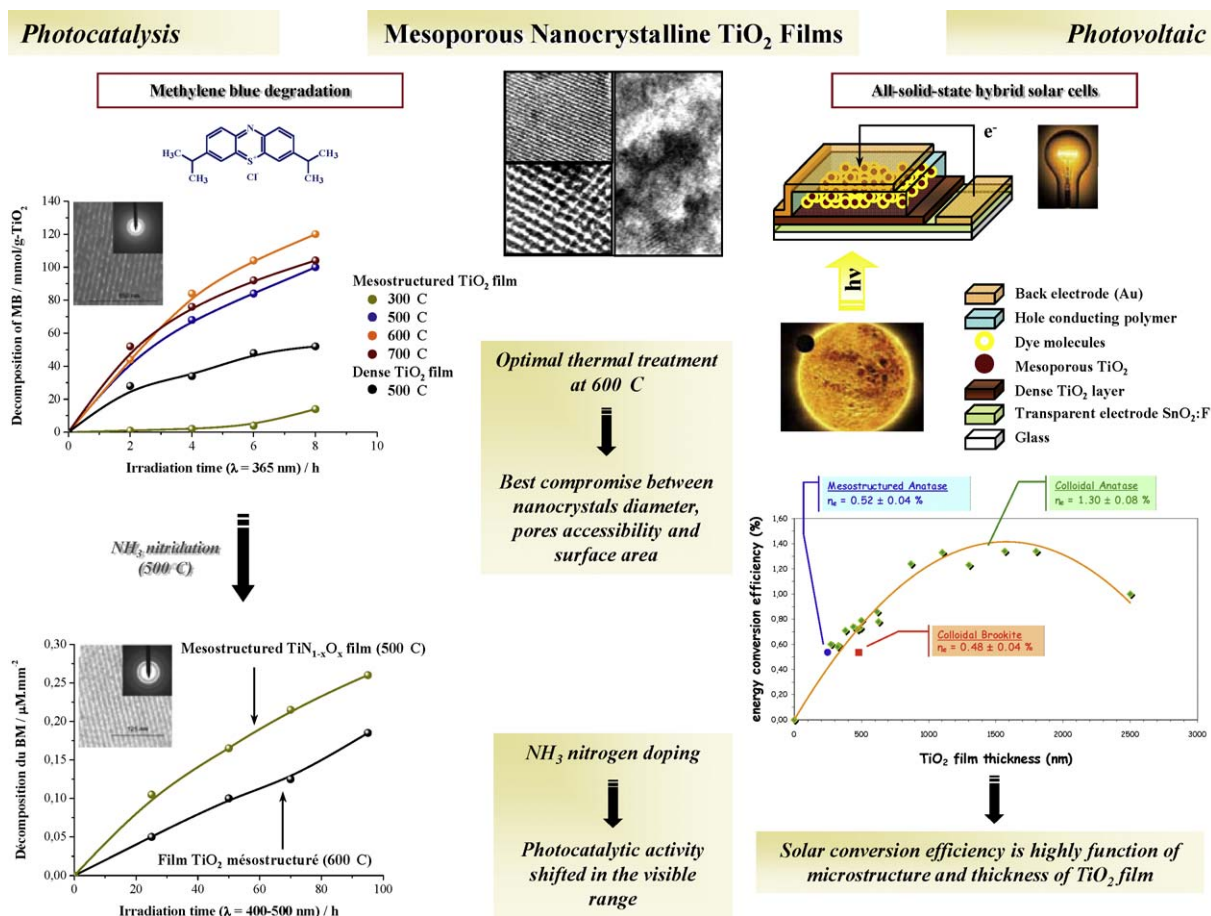


Fig. 9. Left part: Photodegradation of methylene blue over TiO_2 / N-doped TiO_2 films calcined at various temperatures and under UV light or visible irradiation [117,118]. Middle part: Transmission Electron micrograph of a mesostructured anatase film. Right part: A schematic representation of the experimental set-up used for testing mesostructured TiO_2 films [119]. Power energy conversion efficiency for different types of TiO_2 : colloidal anatase-based (◆), colloidal brookite-based (■), and mesostructured anatase-based TiO_2 film (●) as a function of porous TiO_2 layer thickness [119].

5.2.2. Photovoltaic

The literature covering the photovoltaic properties of mesoporous TiO₂ indicates that the solid-pore architecture of the mesoporous films contributes to a facile electron transfer to the collector electrode, to an increase of the electron-hole pair density generated at the hybrid interface and to a better hole-transporting organic material impregnation. These mesoporous films constitute a “host material” for polymers that differ from nanocrystalline films with the same nominal compositions and structure. In these nanocrystalline films, the highest photovoltaic properties for dye-sensitized solar cells (DSSC) are reached for fully nanocrystalline TiO₂ films exhibiting the highest specific surface area (Fig. 9, right part) [120]. These characteristics correspond to the largest polymer-TiO₂ interface. An improvement in solar conversion is possible if the thickness of the TiO₂ mesoporous films is increased and the quality of the hybrid interpenetrating semiconductor nanostructure is optimized. For example, an increase of solar conversion efficient by 50% is obtained for cells containing TiO₂ mesoporous films with a thickness greater than or equal to 1 μm.

5.2.3. Electrochemical properties/Sensing

Mesoporous nanocrystalline thin films offer all the attributes for efficient electrochemical reactions. They exhibit a network of nanoscopic oxides, which can serve as an uninterrupted three-dimensional (3-D) pathway for ions and electrons conduction, and an interpenetrated through-connected mesoporous network which serves as “host material” for electroactive species. In this way, fast ionic or electronic carriers transport in the internal surface area of the mesoporous network may occur. For example, an improvement of proton conduction in mesoporous zirconium phosphate films compared to the ones with disordered porosity has been observed. This behavior is correlated to the high concentration of –OH entities grafted on the pores’ inner surface and the efficient proton diffusion pathways achieved by the organized and well-connected porous network. Furthermore, organic entities grafted at the surface of these mesoporous thin films exhibit a pseudodiffusive electron hopping between the redox species and the inorganic TiO₂ network [121]. The transport of molecules in these mesoporous architectures can, however, be tuned and depends on the nature of the functional groups attached to the pore surface (the length of organic chains, the functionality size or polarity) and on the geometrical constraints including the pore size, the pore orientation and their interconnection [116,122]. This capability is

very interesting for the fabrication of robust membranes or hybrid silica films selective to probes. Indeed, it was observed that the meso-organization of POMTFs offers a better environment for sensing than their corresponding non-organized thin films. Briefly, hybrid POMTF-based optical sensors are characterized by a shorter response time, a whole accessibility of the sensing molecules, a higher sensitivity, an ability to work in both gas or liquid phase without synthesis modifications (due to the large opened and fully accessible porosity), and a response depending on the mesostructure (better with a 3D mesophase compared to a 2D one). Then various optical sensors resulting from the functionalization (one-pot, post-functionalization or combined route [15]) of POMTFs have been elaborated. Scientists synthesized interesting pH, [123,124] O₂, [125] uranyl (UO₂²⁺), [102] explosives (vapor of TNT), [126] and BF₃ (a gas commonly used in semiconductor industries) [127] sensors. Although most of the POMTF-based optical sensors are class II hybrid materials, class I meso-organized sensors have been also reported for the detection of methanol vapor, [128] the determination of pH [129] and the detection of Cu²⁺ in aqueous phase [130]. An alternative way to dye-based sensors has also been investigated. For example, phosphine-stabilized gold NPs encapsulated inside silica POMTFs allowed the detection of thiols and small phosphines due to plasmon band position shifts of gold NPs [131]. Multilayer stacks of TiO₂ and SiO₂ POMTFs functionalized [132], or not [133], were used for the detection of water, alkanes and alcohols via photonic bandgap shifts of these ordered mesoporous Bragg reflectors.

5.2.4. Fuel cells

Mesoporous materials are also used and developed for hydrogen economy. The high surface area-to-volume ratio present in a mesoporous silica network has been used to construct an efficient proton pathway in hybrid organic/inorganic membranes for PEMFC working at high temperature [134,135]. These membranes are constituted of a functionalized mesoporous silica network embedded in a polymer which can be proton conductive or not. The inner surface area of the porous silica network accommodates functional groups i.e. –SO₃H and –PO₃H₂, the connected pore network allow fast transport of hydrated protons and the pore volume serves as a “reservoir” for water. These characteristics permit fast transport for protons throughout the nanoarchitecture while the mechanical strength and gas tightness are ensured by the polymer. Preliminary results have shown that the growth of a functionalized mesoporous silica network in conductive

polymer such as Nafion improves its water retention, its thermal stability and, its proton conductivity at high temperatures [136]. Further, the structure of Nafion[®] is to some extent reproduced in these hybrid membranes, i.e. there is a phase separation between hydrophilic and hydrophobic domains at the micron-scale. Because this phase separation can be tuned through the physical parameter of the sol–gel chemistry and the processing techniques (spray, evaporation, electrospinning), such hybrid organic/inorganic membranes constitute an interesting tool for understanding proton conduction mechanisms at high temperature and low humidity.

5.3. Nanopatterned surfaces by EIMP

TiO₂, Al₂O₃, and ZrO₂ patterns (or masks) composed of ordered nano motifs of various morphologies and typical lateral dimension of less than 60 nm and thickness below 15 nm have been prepared by dip-coating Si-wafer, FTO, glass or even Au-coated substrates in corresponding metal chloride ethanolic solutions in the presence of commercial PB-*b*-PEO or PS-*b*-PEO block copolymer micelles [137–140]. The various nanostructures are obtained by self-assembly during evaporation and are subsequently stabilized at 500 °C. The nano pattern structures and morphologies are usually investigated by combined techniques such as TEM, SEM, AFM, Ellipsometry, Electrochemistry, and GI-SAXS [139]. Here, we chose to illustrate them by AFM images (Fig. 10). Each one of the images is representative of the whole sample surface. They confirm that, by varying the utilized copolymer as well as the chemical and processing conditions applied, various degree of organization and morphologies can be formed at the substrate interface. These various morphologies mainly depend on the solution composition and conditioning that governs the micellisation and the stabilization of the inorganic precursor and the deposition conditions. Most of the work was focused on nanopatterns made of well-ordered and dispersed discoid perforations crossing the thin inorganic layer to give accessibility to the substrate surface, because of its interest in multiple domains of nanotechnology. The present approach is simple, cheap, scalable, and gives high reproducibility without expensive, specialized equipment. On the other hand, chemical and processing conditions must be well controlled in order to optimally achieve highly ordered patterns. Typical requirements are utilizing block copolymers with high molecular weight (i.e. MW > 20.000 g mol⁻¹) and with strong hydrophilicity contrast. These characteristics allows for the micelles to form and stabilize in very dilute

conditions. Hydrophilic chains must ideally be composed of chelating groups, such as PEO, so as to stabilize the inorganic precursors within the shell of the micelles. The principle of pattern formation is illustrated in Fig. 10.

The nanostructure periodicity is associated to the self-assembly of copolymer micelles on the surface, while their thermal decomposition is eventually responsible for the creation of the void motifs such as the nano perforations. Deposition is performed by dip-coating in a dry and warm atmosphere at a withdrawal rate that is adjusted so as to obtain a monolayer of hybrid micelles on the surface. Typical solutions contain around 1% weight of non volatile compounds and require to be deposited between 1 and 2 mm s⁻¹. The coating is thus directly transferred below an IR lamp to be thermally cured. In the first step, the temperature rise up to 200 °C induces inorganic condensation while the PEO polymer chains become less hydrophilic due to a conformation change of the EO units. Both effects promote the depletion of hydrosoluble species (water and inorganic precursors) from the micelle shell region. The inorganic phase condenses between the polymer micelles on the surface of the substrate. Increasing the temperature up to 500 °C causes the complete degradation of the copolymer, leading to the formation of nano cavities at the locations formerly occupied by polymer micelles. The present systems constitute original surfaces bearing ultrathin membranes of inorganic oxide with nanoporations through which the surface of the substrate is accessible. Similar systems can be obtained with polymers using PS-PMMA or PS-PLA block copolymers, [143] the preparation of which is more delicate and longer. Their inorganic homologues are chemically, thermally and mechanically more stable than the polymers which make them complementary materials. According to our investigations, proportion and size of the bare substrate surface area can be tuned between 25 and 75% and 12 and 60 nm in diameter, respectively, by adjusting the chemical and processing conditions. These ceramic based nanopatterns can be seen as novel highly ordered heterogeneous substrates that contain well-dispersed nano sites for heterogeneous nucleation. These sites, or nano beakers, are not only defined by their chemical heterogeneity, but are mechanically confined by the presence of the surrounding ceramic nano walls. When deposited on conductive surfaces, the perforations constitute a nanoelectrode array (NEA) within which polymers (i.e. polyphenol [141]) of metals (i.e. platinum) can be electrochemically and locally generated leading to nanocomposite surfaces. Both membrane and substrate can be of very

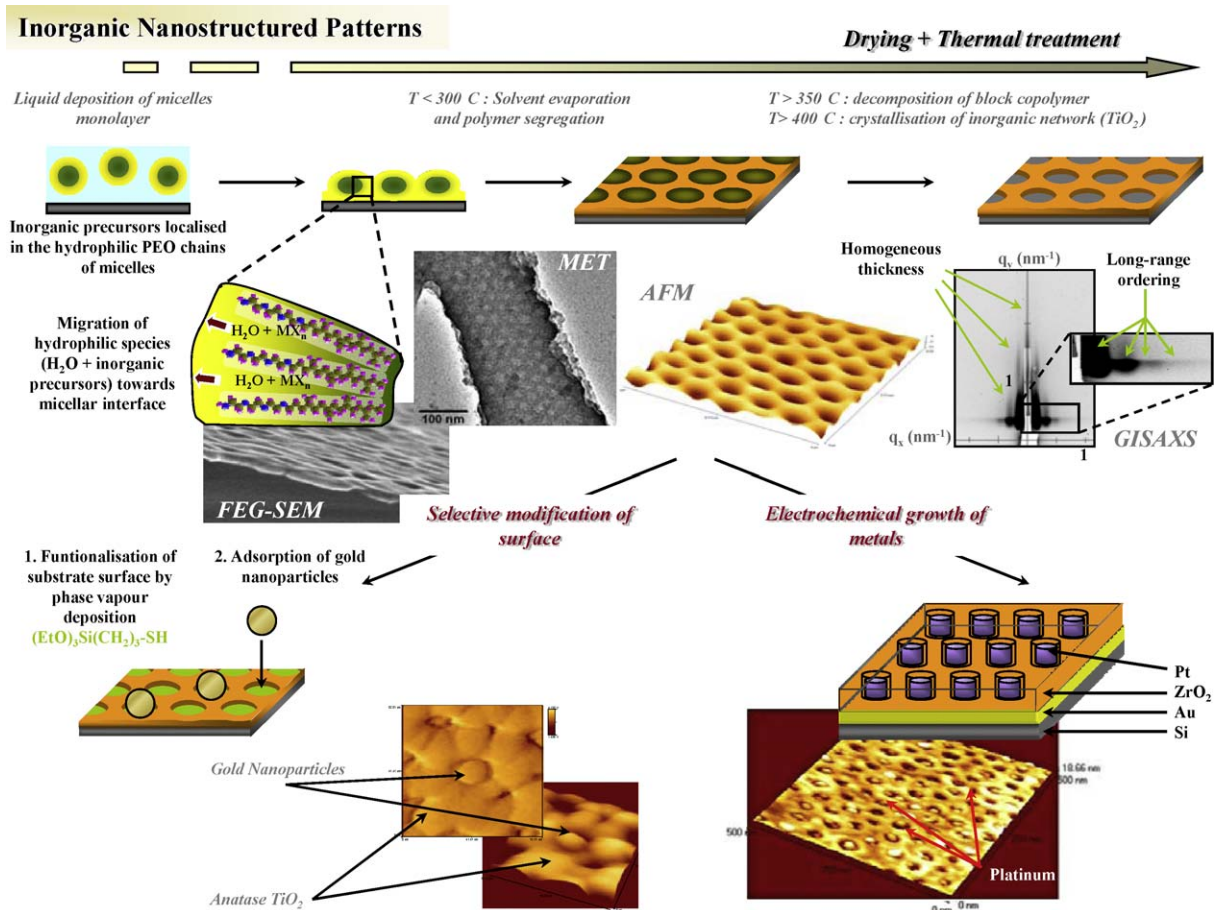


Fig. 10. Scheme describing the formation mechanism of nanopatterned surface by EIMP. AFM, MET, SEM and GISAXS investigation were effectuated onto $500\text{ }^{\circ}\text{C}$ treated TiO_2 nanopattern produced in presence of PB-b-PEO block copolymer onto Si wafer substrates. These revealed that the so-formed nanopattern is homogeneous all over the treated surface, has a thickness of 7 nm, and is composed of circular perforations of 27 nm in diameter which are organised into a 2D compact hexagonal structure of 39 nm of periodic distance. The substrate surface is accessible through the perforations since selective functionalisation with a thiol group promotes the selective addressing of gold nanoparticles inside the perforations. If the substrate is conductive, such as gold, selective reduction of salt can be performed inside the perforation only [15,138–142].

different materials with different surface chemical affinities such as TiO_2 on gold or ZrO_2 on Si wafers. Both materials can be selectively functionalized using appropriated coupling agents such as thiol for noble metals, triethoxysilane for Si-based surfaces, or complexing carboxylic acid or phosphate groups for transition metal oxides. It is thus possible to attach any type of molecule specifically on one of the materials if the molecule is bound to the proper coupling agent. We have, in this way, prepared heterogeneous hydrophilic and hydrophobic surfaces composed of perfluoro groups attached to the inorganic continuous networks [137] or on the second version on the SiO_2 discrete nano patches. Depending on the position of the hydrophobic perfluoro groups, superhydrophilicity (due to 3D enhanced capillarity) or hydrophobicity (due to air

nano bubble entrapment fitting with a Cassie-Baxter model) was observed [142].

5.4. Aerosol route to mesoporous submicronic spheres

Evaporation Induced Self Assembly (EISA) applied to the spray drying process involves a similar structuration mechanism as that described above for the preparation of nanoporous thin films (Fig. 8, right part). Although, in this case, the mother solution containing inorganic precursors, condensation catalyst, structuring agent and volatile solvent is not deposited onto a substrate but is atomized to form an aerosol made of sub-micron size to micron size droplets. The fast drying of these spherical droplets in an oven (the temperature of which

ranges usually between 70 and 500 °C) leads to the generation of mesostructured spherical particles containing all non volatile compounds of the homogeneous mother solution. First applied to the generation of mesostructured silica powders at the end of the 1990s [99], this process is nowadays developing very fast, for it presents numerous advantages for industrial production over conventional solution powder generation processes, such as the batch precipitation:

- it is a continuous process;
- it eliminates time consuming and costly steps such as separation of the powder from the mother solution and washing that produces large volume of effluents to be disposed;
- it is fast (a few seconds are needed to prepare dry mesostructured particles);
- it is easily scalable.

Soon after the initial work proving the feasibility of EISA via the aerosol process [99,144], we investigated in detail the influence of processing parameters over the mesostructuration phenomena that are significantly different from those of coating processes. The final mesostructure obtained by EISA is generally mainly governed by tuning the surfactant to inorganic ratio. Indeed, for CTAB-SiO₂ films for example, the entire range of mesostructures (from cubic to lamellar) has been obtained by increasing the CTAB/SiO₂ molar ratio [78]. However, in spray-drying, the 2D hexagonal structure is systematically encountered in a wide range of CTAB/SiO₂ ratios (0.8 to 0.28) [145,146]. This difference is related to processing parameters and was shown for the first time by SAXS investigations [75]. We designed an unique and very sensitive experiment that involves in situ SAXS characterisation, using a high flux third generation synchrotron (ELETTRA-Italy); This experiment is able to detect meso-order within the aerosol mist (5×10^{-8} g of matter is analysed). By systematically varying the residence time of aerosol in the pre-evaporation chamber, the temperature of the oven (from 25 to 500 °C), the inorganic precursor (TiCl₄ or silicon alcoxide), and the water-alcohol content of the initial solution, we proved that the resting time before heating chamber has no effect on the mesostructuration, while better organisation is obtained with alcohol-rich solvent systems. The tuning of this parameter is of importance since the organic domain structuration has to occur before the inorganic matter condensation rigidifies the structure [77]. Since the evaporation is occurring in a confined environment, alcohol evaporation conditions have to be fulfilled for reaching

structuration (that is the oven temperature has to be higher than the evaporation temperature of the solvent). As a consequence, the critical parameters here are the solvents' partial pressures in the drying chamber (and not the relative humidity observed for film formation at ambient temperature). Finally, the powder being collected by frontal filtration of the aerosol flux, the drying temperature has to be high enough to create rigid submicronic particles in order to avoid the coalescence of the product onto the filter. This rigidifying temperature is very sensitive to the inorganic precursor used and the sol-gel condensation pathway selected [75,147,148].

In parallel, we developed a large spectrum of mesostructured materials (Fig. 11), both for fundamental knowledge development and industrial applications. The simplest metal-oxides based particles with amorphous walls could be obtained by this way: SiO₂ TiO₂, ZrO₂, Al₂O₃ with various mesostructures: 2D-hexagonal, cubic or lamellar [75,107,145,147–149]. These systems were then extended to more complex mixed metal oxides such as SiO₂-ZrO₂, SiO₂-Al₂O₃, SiO₂-P₂O₅. . . [150–152]. In these cases, we observed that a careful tuning of the sol-gel reactivity and degree of condensation of inorganic precursors is needed for achieving a homogeneous incorporation of both metal-oxides. Indeed, whenever the mobility of one inorganic precursor is very different from the other into the surfactant-solvent medium, the drying of the aerosol (starting from the periphery and progressing toward the centre of the droplet) may promote an inorganic-inorganic separation. For example, a gradient of inorganic composition appears for SiO₂-ZrO₂ or SiO₂-Al₂O₃ powders prepared in acidic media whenever more than 10 to 20% of one element is dispersed in the other. The more mobile the precursor, the more concentrated the particle centre. Such inhomogeneity being linked to a diffusion phenomenon, it is more pronounced for big particles than for small ones [151,152].

The concentration gradient created by the solvent evaporation may also be used for promoting hierarchical mesostructures. Accordingly, we used a solution containing a mixture of surfactant, F127 block copolymers and cationic fluorocarbon surfactant IC-11 C₈F₁₇-CH₂-OHCH₂-NH(C₂H₅)₂-Cl to prepared core-shell silica mesostructured particles with a bimodal porous structure [154]. The high surface activity of the fluorocarbon surfactant, the alkyl-fluoroalkyl microphase separation and the solvent concentration gradient associated to the evaporation at the droplet interface were found to be responsible for

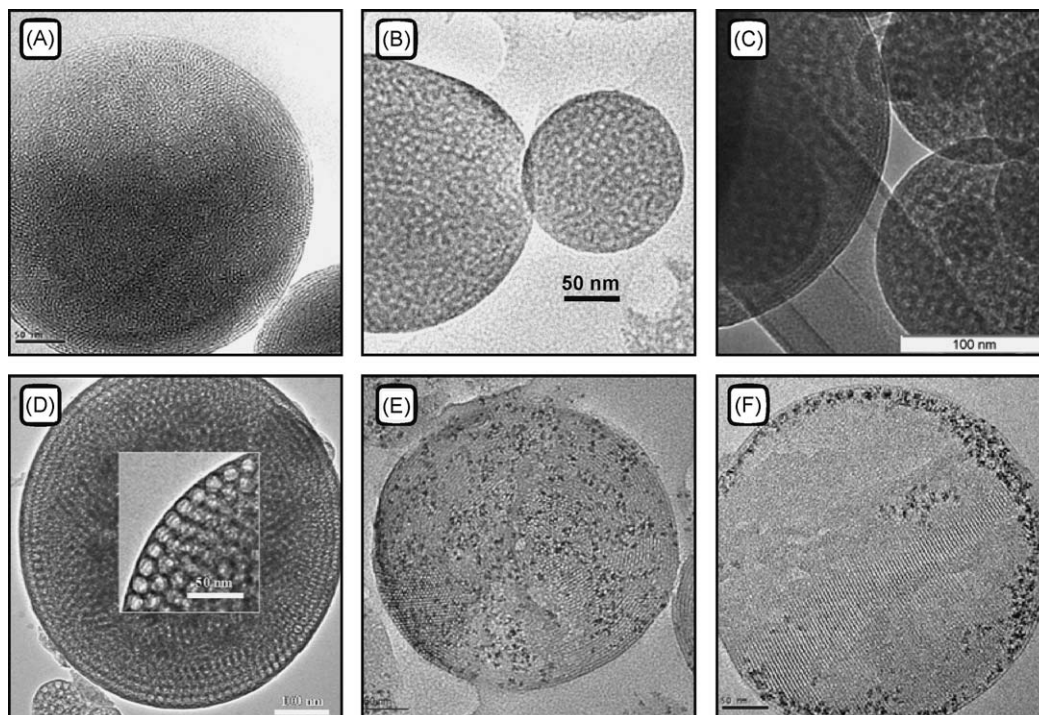


Fig. 11. TEM pictures of mesoporous particles made by aerosol process via EISA. A. Aluminosilicate particles with Si/Al molar ratio of 10 using CTAB surfactant [152,153]. B. ZrO_2 particles treated at 300 °C [148]. C. Hierarchical core-shell silica powders prepared via dual templating strategy using IC 11 and Pluronic surfactants [154]. D. γ -alumina particles nanocrystallised at 900 °C [147]. E. CeO_2 nanoparticles encapsulated in mesostructured SiO_2 particles. F. CeO_2 nanoparticles functionalized by phenylphosphonate species embedded in mesostructured SiO_2 particles [155].

the enrichment of fluorocarbon-surfactant at the particle periphery. This results in the formation of a mesoporous thin membrane at the particle surface, exhibiting a repeating distance of about 4 nm. This layer is due to an earlier micellisation of IC-11 surfactant. In addition, the inner part is also mesostructured but presents much bigger pores, similar to those previously reported for aerosol-generated F127–silica particles (inner pore diameter 7 nm).

By extension with the work done on mesostructured films, we also investigated the crystallisation of the inorganic walls of TiO_2 , ZrO_2 and CeO_2 mesostructured particles [148]. This approach was later adapted for several other transition single and multi metal-oxides compositions [156]. Although, in some cases, the absence of substrate is a handicap for maintaining the mesostructure upon complete nano-crystallisation of the inorganic walls. A solution to the problem was found for generating some mesostructured γ -alumina powders from aluminum chloride precursors by using a specifically designed block copolymer names KLE presenting a very high hydrophobic-hydrophylic contrast and a decomposition temperature higher than 300 °C [147].

In this way, we promoted the condensation of the inorganic precursors $[\text{Al}(\text{OH})(\text{OH}_2)_5]^{2+}$, while favouring the very fast assembly of organic micelles by fast evaporation. The formation of amorphous alumina was then achieved through a post thermal treatment to induce the dehydration of the hydroxide groups. The thermal stability of the organic template (about 150 °C better than usual templates) was crucial here to maintain the mesostructure of the particle. In a second time, a higher temperature treatment lead to the decomposition of the template. A dedicated ^{27}Al NMR study revealed that the temperature treatment has to be raised up to 900 °C to form gamma-alumina nanocrystals. After 30 minutes at this temperature, one obtained fully nano-crystallised powders while maintaining almost intact the particle mesostructure. In all cases, the crystallisation temperature is higher than the one commonly observed for bulk materials. This was attributed to the important contribution of surface energy and to the small thickness of the inorganic walls. These thin inorganic walls delayed the nucleation phenomenon and as for mesostructured thin films prepared by EISA (cf. mesoporous thin films part of this paper).

5.5. Properties of aerosol generated mesoporous submicronic spheres

As mentioned in the previous paragraph, the fundamental study of the EISA performed with the spray-drying process allowed us to much simplify the production of mesostructured submicronic particles. This process becoming very attractive for industrial production we developed several families of materials for very specific applications.

5.5.1. Large pore Aluminosilicates made in Basic media (LAB)

In the first example, we developed in collaboration with the French Institute of Petroleum (IFP) a unique strategy for generating original aluminosilicates materials with exalted acidity for heavy molecules cracking [153]. For this example, the spray-dried solution is sodium-free and only contains clear aluminosilicate precursors stabilised in basic medium, Pluronic F127 template, and tetrapropylammonium hydroxide (TPAOH) as micro-structure directing agent. After calcinations, such unique materials have fully amorphous walls and exhibit a bimodal micro-mesoporous structure with microporous volume ranging from 0.03 and 0.2 cc g⁻¹, mesopores diameters tuneable from 6 and 17 nm, Si/Al molar ratio from 6 to 50, and high surface area (up to 1000 m² g⁻¹), depending on the Al and TPA⁺ contents. Those materials were called LAB for ‘Large pore Aluminosilicates made in Basic media’. The spray-drying process is very advantageous if compared to the precipitation approach since it combined for the first time:

- the direct micellisation and assembly of F127 in basic media (no acidification step is needed to obtain mesopores bigger than 3.5 nm);
- a sodium-free medium (materials are directly in the acidic form after calcinations thus no ionic exchange is needed by contrast with the conventional syntheses of zeolite-seeds made mesostructured materials);
- no zeolite ‘seed’ preformation step is needed (only hydrolysis of silicon and aluminum alkoxides are needed to obtain highly acidic functions at the surface of mesopores).

The aluminum incorporation in the oxide network through those synthesis conditions led to very acidic catalysts compared to standard amorphous aluminosilicates. The iso-surface activity of 8.77 mmol h⁻¹ m⁻² exhibited in m-xylene isomerization by a Si/Al = 12 material is equivalent to the activity of the zeolite based

catalytic reference containing 6 wt% of Y-zeolite (8.64 mmol h⁻¹ m⁻²). Moreover, the study of the m-xylene conversion versus time on stream showed that LAB materials are much less submitted to deactivation by coke formation than this zeolite reference.

Structural origin of this acidity, investigated via FTIR and advanced NMR (²⁷Al)-¹H TRAPDOR and Echo MAS ¹H) proved the presence of very acidic protons close to aluminum centres. This is comparable to mesostructured materials prepared from zeolite ‘seeds’, proving that zeolite nanodomains are not needed to obtain strong acidity exaltation. From an industrial application point of view, this result is very interesting because it proved that a very cheap and simple synthetic strategy leading to amorphous mesostructured materials is sufficient for obtaining efficient aluminosilicate catalysts with exalted acidity and very attractive catalytic properties.

Mesoporous maghemite–organosilica microspheres: a promising route towards multifunctional platforms for smart diagnosis and therapy (Fig. 12). Magnetic vectors for biomedical applications are materials presenting a complex structure coupling a superparamagnetic heart and an organic functional shell needed to improve their dispersal ability, to enhance their chemical stability, and to reduce their toxicity for imaging or therapy purposes. We proposed an innovative concept of a multifunctional “device” with twofold activity for diagnosis and treatment of diseases such as cancer. It deals with an easily made, versatile and biocompatible material which synthesis is based on the dispersion of magnetic nanocrystals (MNCs) in mesoporous silica spheres [157].

The superparamagnetic behaviour of maghemite (γ-Fe₂O₃) NCs together with the high surface area and the possibility of functionalising mesoporous silica allow this composite to combine multiple roles in a single platform. Thus, it could diversely:

- act as a magnetic carrier for biomolecules such as drugs, recognition/blurring agents and specific ligands;
- be localised and followed in the body by magnetic resonance imaging (MRI), since maghemite NCs are known as MRI contrast agents;
- induce an increase of local temperature to kill malignant cells and/or trigger drug release, since maghemite MNCs are known as hyperthermia mediators;
- be surface modified with ligands for targeted drug delivery in specific organs, tissues and cells (molecular imaging, therapy).

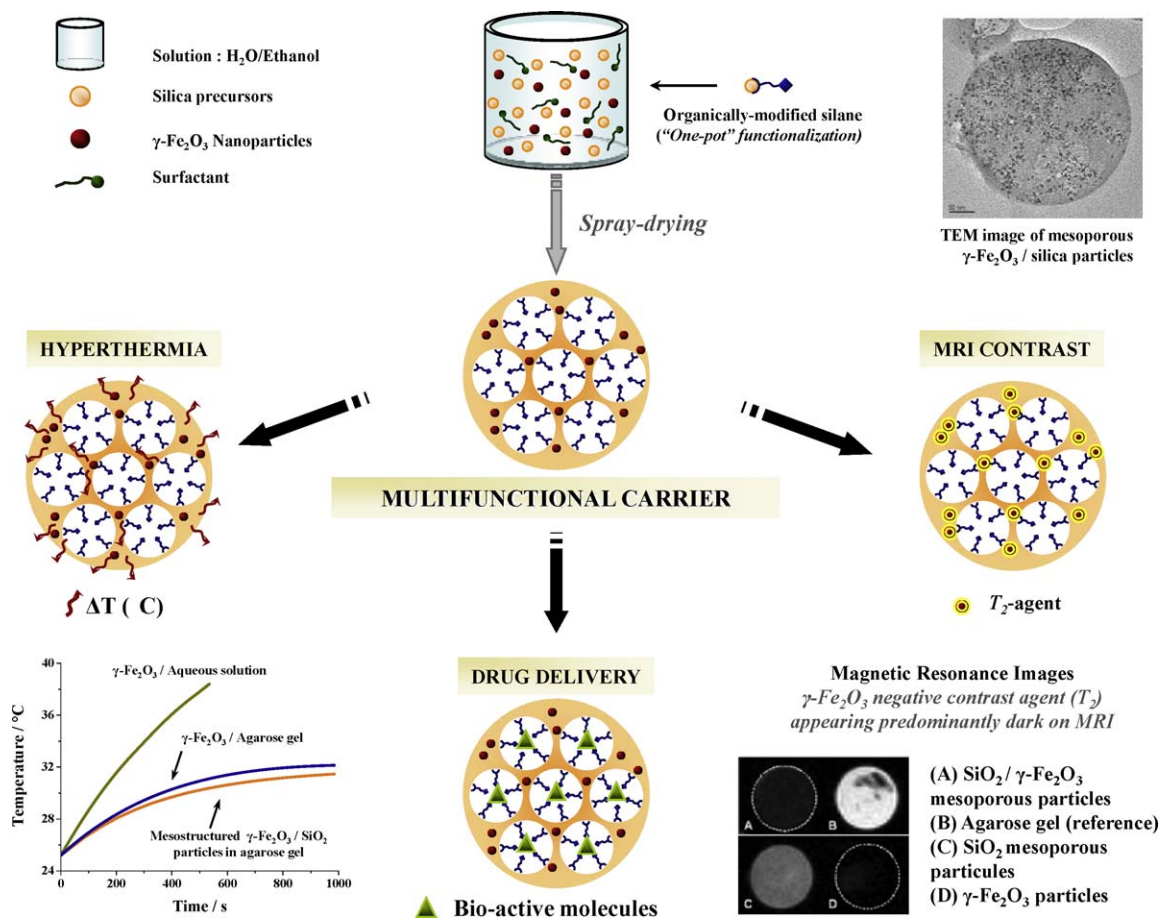


Fig. 12. Mesoporous functionalized silica particles trapping superparamagnetic iron oxide nanoparticles prepared by spray drying exhibit multiple properties: hyperthermia, functionalized porosity for drug carrying and release, and MRI contrasting properties [157].

Our synthesis strategy was a simple and versatile procedure consisting in the spray-drying of a solution containing the magnetic NPs, the inorganic silica precursor, a structuring agent (Pluronic bloc copolymer or CTAB) and an organically modified silane as drug ligand. The solutions were prepared as described in the reference [157]. Briefly, maghemite NPs were mixed with structuring agent and ligand molecules (R-Si(OEt)₃, R = -Ph, C₃H₆-NH₂ or C₃H₆-SH, with ligand/Si molar ratio between 15 and 20%). After spray drying at 350 °C and Soxhlet extraction of the structuring agent, we obtained brown nanocomposite spheres containing intact maghemite NPs (5 to 10 wt%) embedded in a mesoporous silica based matrix. The ordered mesopores diameter is either 2.5 or 8 nm when CTAB or Pluronic is used, respectively. Moreover, these particles exhibit both a high porous volume (0.55 cm³ g⁻¹) and a high surface area (from 400 to 950 m² g⁻¹). This synthesis approach combines many advantages:

- a green and low-cost process that uses biocompatible solvents;
- possible variation of the dimension and structure of the final functional spheres through the dilution of the precursor solution and tuning of the setup conditions;
- absolute control of the final composition (the initial stoichiometry in non-volatile species is retained in the final material);
- mild conditions allowing incorporation of inorganic, organic and biofragile components.

In fact, this direct synthesis using a mixture of TEOS and organosilane as silica precursor allows an effective grafting of any organic functionality onto the silica pore surface. The choice of functionality can thus be adapted to develop specific interactions with drugs or biomolecules by using the chemical reactivity of, e.g., -SH or -NH₂ groups. Finally, we observed that the encapsulation did not affect the maghemite NPs magnetic properties such as:

- in vitro tests of our samples proved very good T2 MRI contrasting agent properties, in good accordance with maghemite NPs properties of similar size described in literature [158];
- hyperthermia property of 5 wt% maghemite vectors was attested (vectors' surrounding medium was heated from 24 to 32 °C in 13 minutes) when submitted to an rf magnetic field (70 kA m⁻¹, 108 kHz).

6. Hierarchically structured materials

Hybrid organic-inorganic materials are increasingly taking their position in the free spaces left between inorganic chemistry, polymer chemistry, organic chemistry, and biology. The controlled design of hybrid organic-inorganic interfaces allows the construction of materials presenting complex hierarchical structures: a particularly interesting challenge for the materials chemists. In particular, the integration between the “chimie douce” driven “sol-gel processing” and “soft matter” is a strong success as both can interact without disrupting its own function. These new approaches where chemistry is strongly coupled with processing have been coined “Integrative Chemistry” [1,3,11,15–17]. They provide the ability to scissor condensed matter at several length scales where final materials and systems will be macroscopically shaped one-dimensional (1D), two-dimensional (2D) or three-dimensional (3D). In general, the main approaches envisaged for multiscale texturation of materials use and combine: nanocasting, cooperative self-assembly (molecular and polymeric surfactants), multiple templating with bigger static (latex, bacteria, virus...) or dynamic templates (breath figures), organogelators templating... [159–161]. A solvent flux driven self-formation of hierarchically structured metal oxides with multiple-scaled porosity based on controlling the hydrolysis and polycondensation rates of reactive metal alkoxides recently reported is also a nice example of dynamic templating [162].

The use of all these various templating strategies combined with “chimie douce” and smart processing methods such as multilayers deposition, aerosols, ink jet printing, electrospinning, foaming (2D and 3D meso-macrocellular foams), contributes to a very attractive field of research. This approach will provide innovative advanced materials, potential candidates for a variety of applications, in the fields of catalysis, optics, photonics, sensors, separation, sorption, electrochemical cells, acoustic or electrical insulation, ultralight structural materials... In particular, materials presenting

multimodal or multiscale porosity present a major interest, for catalysis, fuel cells and batteries, and separation processes, where optimisation of the diffusion and confinement regimes is required. While micro- and mesopores provide the size and shape selectivity the presence of macroporous channels should permit to improve the access to the active sites at the immediate smaller scale, avoiding pore blocking by reagents, carriers and products.

In the following we describe some rational synthetic pathways for generating complex porous architectures. The main examples will be selected in research areas in which the “Paris hybrid materials group” is contributing (Fig. 13).

6.1. Multiple templating

Monodisperse spherical hollow NPs of mesoporous silica featuring mesopores with a radial orientation in the silica shell can be synthesized via a dual-templating method. Specifically designed polystyrene latexes with anionic or cationic surface charges acted as the core templates, while cetyltrimethylammonium bromide served as a cotemplate to structure the mesopore formation during tetraethoxysilane hydrolysis/condensation. The particles were well-separated and presented homogeneous mesoporous silica shells. Average particle diameters were less than 200 nm, and the particles displayed high values of specific surface area and pore volume. The shell thickness and the hollow core diameter could be tuned independently while the radial pore structure was preserved. Nitrogen adsorption-desorption isotherms proved that the central cavity was only accessible from the external medium through the radial mesopores of the shell. Consequently, these particles gather the advantages of a well-defined structure, straight penetrating channels across the silica shell, and a high accessible porous volume of the central core. Hybrid materials were synthesized via grafting polymer chains from the surface of these ordered mesoporous silica particles via surface-initiated atom transfer radical polymerization of methyl methacrylate or styrene. The perfectly controlled polymerizations of MMA and styrene in the homogeneous medium via ATRP allow obtaining bimodal porous particles with a multiscale functionality control. In the future, this conceptual approach will be transferred to systems combining these ordered mesoporous silica particles with thermo- or pH-sensitive polymers making these hybridized mesoporous vectors interesting candidates for any storage and/or controlled release applications [166,168].

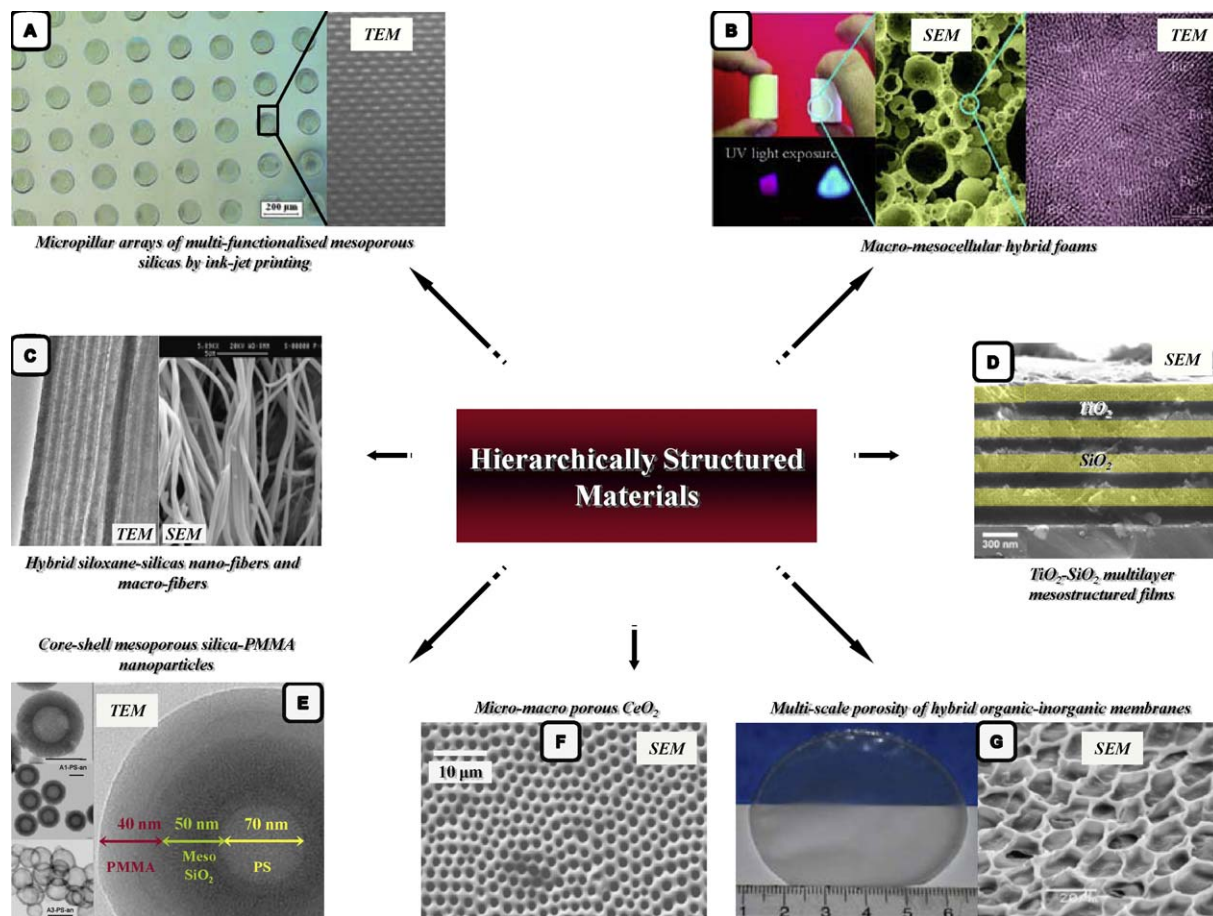


Fig. 13. Illustration of the multi-scale porosity of the present hybrid organic-inorganic membranes. A. Micropillar arrays of multi-functionalised mesoporous silicas by ink-jet printing, [163]. B. Macro-mesocellular hybrid foams [164]. C. Hybrid siloxane-silicas nano-fibers and macro-fibers [34]. D. TiO_2 - SiO_2 multilayer mesostructured films [165]. E. Core-shell mesoporous silica-PMMA nanoparticles [166]. F. Micro-macro porous CeO_2 [33,167]. G. Multi-scale porosity of hybrid organic-inorganic membranes [135].

6.2. Dynamic templating

6.2.1. Controlled phase separation

Multiscale texturation methods that take advantage of phase separation processes have also been described. In this approach, the precipitation of the inorganic phase can be performed within a solvent or mixtures of hydrosoluble/hydrophobic polymers. Hierarchically-controlled morphology is attained by controlling gelation and precipitation processes; the phase separation step generally occurs via a spinodal decomposition which is frozen by the inorganic polymerisation. Indeed Mesoporous-macroporous silica has been obtained by Nakanishi et al. [159] in an original and simple fashion by adjusting sol-gel hydrolysis/condensation kinetics and solvent-mineral polymer interactions. Macroporosity can be controlled by inducing a phase separation of hydrosoluble polymers in parallel to a sol-gel

transition. Mesoporosity can be controlled by solvent exchange and treatment in alkaline conditions. These silica phases are being developed as highly efficient separating medium in chromatography columns.

Recently, we have proposed an approach to form transparent hierarchical hybrid functionalized membranes using in situ generation of mesostructured hybrid phases based on organically modified silica inside a non-porogenic hydrophobic polymeric (PvBu) host matrix. Following this new route, different macro-organizations can be obtained with a specific mesostructure, depending on the surfactant-polymer-solvent affinities and also on one-pot synthesis conditions [134]. The mesostructured component is prepared by EISA of inorganic and hybrid precursors in the presence of surfactant, water, solvent, the organic polymer host and catalysts. During solvent evaporation, self-assembly of the mesophase and phase separation of the

polymeric host occur simultaneously. The control of the multiple affinities existing between organic and inorganic components allows designing the length-scale partitioning of hybrid nanomaterials with tuned functionalities and desirable size organization from the angstrom to the centimetre. The functionalization of the mesoporous hybrid silica component yields membranes having good ionic conductivity, therefore opening interesting perspectives for the design of solid electrolytes, fuel cells and other ion-transport microdevices.

Moreover, hybrid membranes made of a Nafion host matrix have been developed using the same concept and following a similar procedure. Organic-inorganic hybrid membranes of Nafion and mesoporous silica containing sulfonic acid groups were synthesized using the sol-gel process with the goal of increasing the proton conductivity and water retention at higher temperatures and lowering relative humidities as well as improving the dimensional stability. These hybrid membranes were prepared via in situ co-condensation of tetraethoxysilane and chlorosulfonylphenylethyltrimethoxysilane via a self-assembly route using organic surfactants as templates for the tuning of the architecture of the silica or hybrid organosilica components. These hybrid membranes containing functionalized silica showed a higher ionic exchange capacity and greater water management than standard Nafion. The hybrid membranes exhibit improved proton conductivity at 95 °C and over the whole range of relative humidity in comparison to recast Nafion and Nafion 112 membranes [136]. Owing to the promising membrane behaviour under low humidity level and higher operating temperature conditions, large hybrid silica-Nafion prototype membranes have been prepared and tested in a real fuel cell. Such experiments demonstrated a reliable increase in current density of 15% under severe conditions (low humidity level at 50% and gas pressure H₂/air at 1.5 bars) compared with commercial Nafion membranes [134].

6.2.2. Breath figures as smart templates

Among the diversity of templating strategies available, the use of “breath figures [BF]” (BFs, the fog created by exhaling on a cold surface) as a method to generate texture on the micrometer scale has gained interest [33,35,167,169,170]. Honeycomb-like macroporous coatings can be patterned on the micrometer scale under high humidity conditions by casting volatile solvents containing organic, inorganic, hybrid polymers or particles. For example, BFs can be obtained by using, in the presence of moist air, a solution of functional hybrid NBBs, in CHCl₃, or THF. Evaporation of the solvent leads to a decrease of the air-liquid interfacial

temperature of the cast liquid. This evaporative cooling of the solvent induces the condensation of micrometer-sized water droplets on its surface. The condensed water droplets are transferred into the cast liquid by convection of the solvent and assemble in ordered arrays on the liquid surface. After evaporation of the solvent and the water droplets, which act as a template, a honeycomb-like patterned film can be obtained. The walls of this macroporous membrane are constituted of assembled NBBs which create, via controlled sintering, a nanoporous network. Moreover, the adjustable size of the nanobuilding unit permits an easy tuning of the mean size of the nanoporosity between 1 and 50 nm.

The use of suitable NBBs as precursors with a tailored inorganic core and surface functionality presents many advantages:

- a better definition of the inorganic component with tailored structure and size-dependent properties;
- a lower reactivity towards chemicals than molecular agents;
- an already condensed state allowing for the minimization of sintering and, hence, control of textural porosity;
- nanometric, monodisperse, and nanocrystalline NBB components, which facilitates the characterization of the final materials.

We have shown that this strategy is general, simple, versatile and allows the assembling of a large variety of structurally well-defined NPs with very different chemical compositions (silica, transition metal or rare-earth oxides (TiO₂, CeO₂), metals (Co), chalcogenides (CdS) into complex porous architectures.

In particular we have shown that the chemical strategies offered by the coupling of functional NBBs, made of surface hybridized NPs (polymer or surfactant-modified NPs of SiO₂, TiO₂, CeO₂, Co, CdS...) and breath figures processing allows for the development of porous materials with hierarchical porosity [33,167,169]. As an example, honeycomb-like macroporous membranes or films made of metallic oxides, metals, or chalcogenides having mesoporous walls have been easily obtained (Fig. 13). The combined use of solvent evaporation induced BF of ceria NBBs /PBLG (polybutyl L-glutamate) THF solution permits the production of polymodal microporous-macroporous CeO₂ membranes with surface areas of 150 m²/g. These approaches can likely be extended to the formation of polymodal porous membranes based on zeolites, carbides, nitrides, inorganic-organic (or bio-) hybridized NPs. . .

More recently we have designed meso- and macropore architectures in hybrid organic-inorganic membranes by combining surfactant and breath figure templating [135]. The membrane architecture is made of a three-dimensional interconnected network of hydrophilic mesostructured SiO_2 carrying acidic functionality ($-\text{SO}_3\text{H}$) in an inert/uncharged thermostable polymer, PVDF-HFP. The uncharged (hydrophobic) polymer which surrounds the three-dimensional mesostructured hybrid SiO_2 network restricts SiO_2 network swelling in water and provides mechanical strength to the membrane. The mesostructure in the hydrophilic silica network affects properties critical to the H^+ -conduction performance: they exhibit an enhanced surface area to accommodate the proton conducting functional groups together with facilitated transport properties. Additionally, generating macropores by the breath figure templating creates micron-sized cavities at the surface of the hybrid membranes that:

- increase the surface area at the electrode/electrolyte interface limiting the overall interfacial resistance;
- control water management at the cathode interface preventing both flooding and drying of the membrane electrode assembly.

Furthermore, it does also change the hybrid interface through a separation of the hydrophilic and hydrophobic domains.

The effect of the internal structure – mesopores and the quality of the hybrid interface – translates into different conductivity values depending on the temperature and the humidity. This indicates that a blend of order in the pore and a controlled phase separation between the hydrophilic and the hydrophobic domains is needed to maximize the proton conduction. The “sol-gel” derived route, high proton conductivity and the ability to create hierarchical porosity make this design advantageous for low temperature PEMFC fuel cells. These concepts can be extended to other applications such as batteries, sensors or ion-exchange membranes.

6.3. Organogelators templating

Low molecular-weight organogelators are molecules capable of forming thermoreversible physical (supramolecular) gels at very low concentrations (ca. 10^{-3} mol dm^{-3} , typically lower than 2% w/w) in a wide variety of organic solvents. Upon gelation, the organized self-assembly of these molecules results in the formation of highly anisotropic 3-D structures,

mostly in the shape of fibers, but also ribbons, platelets, tubular structures or cylinders. Since the first report by Shinkai et al. [32,34,171] in 1998, supramolecular organogels (or hydrogels) have been successfully used as templates to direct the growth of a wealth of inorganic (commonly oxide-based, but also some metals and semiconductor chalcogenides) and also hybrid (organic-inorganic) nanofibrous materials.

Combined with soft chemistry-based approaches many organogelators have been already used as templates for materials transcription [34]. The most important processing methodologies that are available for materials transcription through organogel templating are co-assembly, post-transcription, or self-templating procedures. The main types of intermolecular interactions responsible for the gel-phase formation and some of the principal variables governing the gelation process and controlling the obtained fibrous morphologies (fibers, rods, ribbons, helices, tubes, etc.) have been recently reviewed [32,34]. In the group, we have designed micronic and mesoporous fibers of different inorganic (silica, alumina) [172] and organic-inorganic hybrid materials [173]. In particular, the growth of hybrid organosilicas supporting different functional moieties has been successfully directed through the use of templating strategies with organogel assemblies based on anthracenic molecules (Alkoxy-anthracenes, Alkoxy-Phenazines). By performing in situ the sol-gel condensation reactions of organo-trialkoxysilanes or organosilsesquioxanes during the assembly of the organogel phase, it has been possible to prepare nanofibrous organosilica replicas having pendant organic functionalities: mercaptopropyl, methacrylate, ethylenediamine, dinitrophenylamine. In the case of using the more amphiphilic phenazine derivative as template, the hybrid organosilicas (supporting the phenyl, amino, mercapto, methacrylate, diamino, and dinitrophenylamino moieties) were synthesized by templating the co-condensation between tetraethyl orthosilicate and the corresponding organotrialkoxysilanes (PTES, APTES, MPTMS, MAPTMS, *en*PTMS and DNPAPTES, respectively), mainly under acid catalyzed conditions.

The templating of fibrous morphologies was successful in all cases, irrespective of the different hydrophobic or hydrophilic character of the employed organotrialkoxysilanes, and the morphologies were preserved after removal of the organogel template. Noteworthy, the templated hybrid organosilica containing phenyl moieties (the most hydrophobic) consisted of highly intertwined fibrous bundles, 5–20 μm thick, resulting from the aggregation of much thinner

nanotubes (Fig. 13), whereas the protonated amine sample was formed by a mesh of straighter and elongated fibrous ribbons (*ca.* 5–10 μm thick) also arising from the aggregation of much thinner, and this time perfectly co-aligned, fibrils. In the case of mercapto and methacrylate samples (with intermediate hydrophobic or hydrophilic character) both types of morphologies (intertwined fibrous bundles and entangled ribbons) were observed, with a predominance of ribbon-like regions.

Recently pH-sensitive pyridine-based gelators (Amino acid-based gelators such as [N-nicotinoyl-L-valyl]propylenediamine) and -[N-benzoyl-L-valyl]propylenediamine) have been found to be flexible and efficient templates for the transcription of nanofibrous helicoidal silicas fibers [174]. The morphology and aggregation degree of silica nanofibers and nanotubes (30–60 nm thick, with 3–10 nm inner channels) could be tuned by simply adjusting the pH conditions through the use of “in situ” formed organogels. Interestingly, silica nanotubes with larger inner mesoporous channels (5–35 nm) were obtained by using a “postdiffusion” route instead of the conventional “one pot” or in situ strategy.

6.4. Building block assemblies for photonic band gap materials

6.4.1. Latex games

The capability of monodisperse particles of poly (methyl methacrylate) and of styrene copolymers for self-assembling in close-packed three-dimensional ordered arrays can be used to design inorganic materials exhibiting properties of photonic crystals. Indeed, 3D photonic crystals can be obtained by filling the voids (between the latex micro-spheres) of closely packed assemblies of polystyrene microspheres with typical diameters between 0.1–2 μm with an inorganic sol-gel derived high refractive index metallic oxide [175,176].

The improvement of this strategy was made via a simple method that permits one to obtain triple-scale-hierarchically ordered silica. This method, based on the use of PDMS micromolds, latex NPs and amphiphilic molecules has been developed by Yang et al. [161]. The micromoulding is performed by patterning a PDMS template, and the submicronic texture is again formed by packed PS spheres. The mesoporous structure is generated in the voids of the PS colloidal crystal, via a cooperative self-assembly of the inorganic species and the poly (ethylene oxide) block copolymers (PEO-PPO-PEO) template.

6.4.2. Multilayers deposition of POMTF

Today a large number of strategies have been developed to create periodically organised mesoporous thin films (POMTFs) with a variety of oxide frameworks, compositions, organic functions [15,132,165]. These POMTFs monolayers can be synthesized reproducibly with perfectly tuned features in the mesoscopic or molecular scales. These single-layer films can thus be considered a “functional building block” for the construction of more complex architectures, which can give access to new properties arising from order in space at different length scales. Recently Soler et al. [132,165] developed a smart strategy for the controlled design of high-optical quality one-dimensional photonic crystals built using functional mesoporous thin films as building blocks (Fig. 13). Multilayer stacks of mesoporous films ($\text{SiO}_2/\text{TiO}_2$) give rise to environment-sensitive Bragg reflectors for which the tuning of optical properties can be achieved by changing the composition or porosity of the slabs or the introduction of planar defects. Sorption or capillary condensation of molecules into the pore system results in a 10–40 nm photonic bandgap (PBG) shift. The optical response of these colored mesoporous multilayers can be tuned through the selective introduction of organic functional groups added to the pore surface. This change in the response allows for tuning the selectivity towards small-size molecules [132,165]. From the in situ analysis (*optical response combined with poro-ellipsometry*) [113], it has been shown that the changes in solvent uptake that occur in each type of layer in the ensemble at ambient pressure modify the optical responses of the multilayer system. These modifications depend on the pore size, the wall nature, and the surface features of the multilayer components. However, for the ultimate tailoring of the optical response, the collective as well as the individual behavior of each monolayer must be taken into account because the interaction between neighboring layers play an important role. This work opens the possibility of performing selective spatial adsorption, chemical reactivity, and directed mass transport in these complex multiscale architectures. It constitutes one of the first examples of the great potential of these hierarchical structures [132,165].

6.5. Aerosol processing

As previously mentioned the mild synthetic conditions of the EISA method allow the incorporation of inorganic, organic or even bio components with interesting and assorted properties. An interesting

example of gold metal or metal oxide NPs within mesoporous silica spheres has been obtained through “one-pot” synthesis (by spray-drying) in our research group. These materials exhibit functional hierarchical structures composed of several components with tuneable size: micronic or submicronic inorganic spheres (sol–gel derived silica or TMO having between 0.1–10 μm in diameter), mesopores (which diameter range 3–10 nm) and all kind of NPs (2–10 nm in diameter). They have been prepared following the protocol for the synthesis of mesostructured pure silica microspheres, but introducing the dispersed latex beads, gold or metal oxide NPs (M_xO_y) into the initial sol before the spray-drying process. A typical solution can be composed of the silica precursor (TEOS), a template (surfactants), the metal oxide NPs (CeO_2 , Fe_2O_3 . . .) or the desired metallic NPs (Au, Pd . . .), a volatile catalyst, and a volatile medium (water, ethanol). This initial sol must be perfectly transparent and stable in order to avoid the clusterization of the introduced NPs precursors.

The control of particle localisation can be achieved thanks to an adequate functionalisation of NPs (with a specific R function) and an accurate control of the spray drying process parameters. The observation of the spatial repartition of the NPs within the spherical submicronic particles can be made on microtomed samples by Transmission Electron Microscopy. The controlled integration of ceria NPs into hierarchically-structured mesoporous SiO_2 microspheres is illustrated in Fig. 11. Non functional 30 \AA size nano-ceria particles can be homogeneously distributed in the mesoporosity of the silica microspheres obtained through the block-copolymer template (Fig. 11E) while phenyl capped nano-ceria is accumulated in a belt close to the surface of silica microspheres (Fig. 11F). However, a deeper understanding of the complex self-assembly mechanism, which drives the different species to co-assemble into tailored architectures, is necessary in order to achieve optimal spatial distribution, surface accessibility, and functionality [75,145,148,154].

6.6. Ink jet printing and cooperative self-assembly

Another possible strategy to obtain hierarchically structured coatings can be achieved by combining silica-surfactant self-assembly with processing routes such as pen lithography or ink-jet printing [123, 163,177]. Previous experiments have demonstrated that the ink-jet printing process allows building 3D ceramic structures layer-by-layer, with the aid of a computer design by depositing ceramic suspension microdroplets

ejected via a nozzle [178]. In a similar approach, Lejeune et al. demonstrated the feasibility of preparing 3D fine-scale micro pillar arrays of mesoporous silica, with pillar sizes around 60 μm in diameter and a few 100 μm high, by coupling ink-jet printing and the EISA processes. The precursor solutions were based on chemical compositions developed for the deposition of mesoporous silica based films by dip-coating (inorganic and hybrid alkoxide precursors, acidic water and an ionic or non ionic surfactant) [15]. Controlling the ink jet deposition parameters and precursor hydrolysis made it possible to obtain mesoporous silica with a Pm3n cubic structure, using CTAB, or an Fmmm orthorhombic structure, using a nonionic surfactant as F127. The addition of hydrophobic organosilane $\text{F}_3\text{C}(\text{CF}_2)_5\text{CH}_2\text{CH}_2\text{Si}(\text{OC}_2\text{H}_5)_3$ leads to the most regular and well-defined three-dimensional microdot array with a constant diameter of 155 μm and a regular space of 250 μm (Fig. 13). Recently, this strategy was extended to hybrid organosilica with tuneable functionalities [179]. Such hierarchically patterned coatings based on inorganic or hybrid structures could be used to develop hyperhydrophobic or hyperhydrophilic coatings, and catalytic layers. Moreover, the possibility to use an ink jet multi-printing head system to graft in “one pot” different organic functionalities from a dot to another opens the way to the fabrication of highly sensitive miniaturized sensors. They would be based on multi arrays of functional mesoporous dots and could be used in many different fields (heavy metal trapping, artificial noses, molecular recognition applied to the antibody detection for the diagnostic of infections).

6.7. Foaming processes

6.7.1. 2D mesomacrocellular

2D inorganic porous films can be easily generated by the controlled combination of condensation, crystallization, and sintering of an inorganic phase with the foaming associated to the gas formed upon decomposition of organic components. For example, such a strategy allowed us to process high-quality transparent ultralow-refractive-index and ultralow-dielectric-constant thin films which are important for designing smart devices and systems for microoptics and microelectronics (for example, multilayer structures, optical resonators, photonic crystals, Cu interconnects, insulating layers and so on). The method is very simple and robust. It allows one to prepare MgF_2 -based optical thin films exhibiting refractive indices ranging from 1.08 to 1.2 and ultralow dielectric constants ($k_{100\text{ kHz}} = 1.6$). The coatings were deposited on solid substrates through

chemical solution deposition from a single and extremely stable (up to few years old) sol–gel solution composed of magnesium acetate and trifluoroacetic acid dissolved in a mixture of ethanol and water. The generation of the porosity responsible for the ultralow refractive indices of these materials is triggered by the thermal decomposition of the metallic precursor ligands. The resulting nanobubbles of gas are then frozen-in by the thermally induced condensation and partial crystallization of the mineral network around them. Such a process is governed, and can be perfectly controlled, by the heating rate and the atmospheric water content applied during calcination, through which nanobubble size, quantity, and the material's chemical makeup are tuned. Moreover, the process used to prepare these nanomaterials is also well suited for industrial production requirements such as scaling up, processing conditions, solution conditioning and storage. The resulting vesicle-like porous materials demonstrate a range of tunable compositions with varying refractive indices and combine good mechanical properties with high chemical and thermal resistance [95,180].

6.7.2. 3D mesomacrocellular foams

One way to obtain hierarchically organized inorganic and hybrid materials consists in the use of either direct concentrated aqueous emulsions, [176] surfactant/colloids stabilized aqueous emulsions [181] or through gas foaming processes combined with sol–gel chemistry [182]. An original approach to hierarchically structured inorganic and hybrid materials was recently developed by Backov et al. [164,183] who combined controlled polymerisation of metal alkoxide precursors with emulsion and lyotropic mesophase templating modes. The general aim was to develop a new process for obtaining inorganic and hybrid macrocellular silica monoliths with a good control over the final macroscopic cell sizes and morphologies by tuning the oil volume fraction of the starting emulsion. This new series of inorganic or hybrid silica porous networks were labelled Si(HIPE) or Organo-Si(HIPE) respectively (Fig. 13), in reference to the first generation of porous organic polymers obtained through the use of concentrated reverse emulsions, known under the acronym “polymerized High Internal Phase Emulsion” [184]. This new class of grafted organo-Si(HIPE) are robust centimetric monoliths with both macroporous and mesoporous highly interconnected networks. This family of functional 3D monolithic foams was first tested in the fields of catalysis and adsorption. Indeed, Organo-Si(HIPE) loaded with internal palladium

particles via heterogeneous nucleation offer good turnovers and cycling performance. For instance, the Pd@mercapto-Si(HIPE) matrix allows for 96% of Heck coupling catalysis yield during seven cycling tests. The Pd/iodobenzene molar ratio was settled at 0.004 and 0.002. The turnover number (TON) and turnover frequency (TOF) addressed with these new monolith catalysts are reaching values comparable with those obtained with powdered commercial catalysts. Considering the fact that the catalysts in use are not powders but rather monoliths bearing hierarchical porosities, the series of Pd@organo-Si(HIPE) compounds combine heterogeneous catalysis efficiency and facile recyclability as catalyzed species and catalyst supports can be easily separated by a simple removal of either the monolith or the solution from the reaction media.

Also, organosilica-based hybrid monoliths exhibiting a hierarchically structured bimodal porous structure with grafted chelating functionality (malonamide, benzoylacetone) can be efficiently loaded with lanthanides to give Eu^{3+} @ γ -malonamide-Si(HIPE) and Eu^{3+} @ β -diketone-Si(HIPE) hybrid foams. Optical properties of these versatile materials with macro- and microporosity have been addressed throughout their absorption and emission spectra along with their relaxation luminescence properties. Eu^{3+} containing Organo-Si(HIPE) materials are strongly luminescent foams. This new class of foams clearly opens a land of opportunities for the development of promising applications in catalysis, optics, sensors, chromatographic supports, and so forth. Beyond, several promising developments associated to the field of materials dedicated either to energy or biomass valorisation are under investigations [185].

7. Conclusion

Organized nanostructures and nanostructured materials often exhibit improved or even unique physical, chemical, and other properties. These specific properties are achieved through the design and the control of hybrid organic-inorganic interfaces [36]. A new class of hierarchical structures has appeared after the first phase initiated by the sol–gel community. This new field of research is grounded on the comprehensive study of the material properties from the molecular to the nanometric or micronic scales. These were mainly dictated by applications from biological and chemical sensing, catalysis, energy, selective separation to optical communications, etc. Many of these advanced inorganic and hybrid organic-inorganic materials synthesized via

“chimie douce” are at the “cross-roads” of inorganic chemistry, polymer chemistry, organic chemistry, and biology. Biomimetism and bioinspiration are smart tools for the design of innovative materials and systems that are strongly inspiring the materials chemistry community. Indeed, materials found in nature combine many wonderful features such as sophistication, miniaturization, hierarchical organizations, hybridation, resistance and adaptability. Elucidating the basic components and building principles selected by evolution to propose more reliable, efficient and environment respecting materials requires a multidisciplinary approach. Bio-inspired strategies are included in a wider emerging new field coined “bio-inspired or integrative materials chemistry” [1–4,11,16,17,186]. This field is opening not only new lands for innovative research but should also motivate or even give birth to a passion for research in young scientists.

Acknowledgements

Jacques, please receive many acknowledgments from all of us, because with “chimie douce” you opened the gate towards a new galaxy of materials.

CS would like to acknowledge all PhD students and postdoctoral researchers who worked with the hybrid materials group of the LCMCP for their contribution and enthusiasm to this wonderful land of research namely: M. Nabavi, S. Doeuff, P. Griesmar, M. Kallala, M. IN, F. Banse, B. Lebeau, J. Blanchard, N. Steunou, B. Alonso, E. Scolan, A. Bouchara, B. Julián-López, F. Mammeri, F. Cagnol, F. Goettmann, A. Coupe, F. Pereira, A. Qualch, L. Bisson, N. Chemin, S. Pega, M. Kuemmel, T. Frot, G. Soler-Illia, E. Crepaldi, M. Llusar, G. Fornasieri, Y. Sakatani, Y. Castro, E. Martinez, J. Bass, E. Lancelle, J. Allouche, O. Sel.

References

- [1] C. Sanchez, H. Arribart, M.M. Giraud Guille, *Nature Materials* 4 (2005) 277.
- [2] G.A. Ozin, *Chemical Communications* 6 (2000) 419.
- [3] S. Mann, *Biomimetic Materials Chemistry*, Wiley-VCH, Weinheim, 1997.
- [4] S. Mann, *Angewandte Chemie-International Edition* 39 (2000) 3393.
- [5] R.P. Gomez, C. Sanchez, *New Journal of Chemistry* 29 (2005) 57.
- [6] J. Livage, *Le Monde* (1977) October 26th;
J. Livage, J. Lemerle, *Annual Review of Materials Science* 12 (1982) 103;
J. Livage, *Chemistry of Materials* 3 (1991) 578.
- [7] J. Livage, M. Henry, C. Sanchez, *Progress in Solid State Chemistry* 18 (1988) 259.
- [8] D. Avnir, T. Coradin, O. Lev, J. Livage, *Journal of Materials Chemistry* 16 (2006) 1013.
- [9] C. Sanchez, F. Ribot, *New Journal of Chemistry* 18 (1994) 1007.
- [10] C. Sanchez, G.J.A.A. Soler-Illia, F. Ribot, T. Lalot, C.R. Mayer, V. Cabuil, *Chemistry of Materials* 13 (2001) 3061.
- [11] G.J.A.A. Soler-Illia, C. Sanchez, B. Lebeau, J. Patarin, *Chemical Reviews* 102 (2002) 4093.
- [12] S. Mann, S.L. Burkett, S.A. Davis, C.E. Fowler, N.H. Mendelson, S.D. Sims, D. Walsh, N.T. Whilton, *Chemistry of Materials* 9 (1997) 2300.
- [13] C.G. Goltner, M. Antonietti, *Advanced Materials* 9 (1997) 431.
- [14] D. Avnir, D. Levy, R. Reisfeld, *Journal of Physical Chemistry* 88 (1984) 5956.
- [15] C. Sanchez, C. Boissiere, D. Grosso, C. Laberty, L. Nicole, *Chemistry of Materials* 20 (2008) 682.
- [16] R. Backov, *Soft Matter* 2 (2006) 452.
- [17] E. Prouzet, S. Ravaine, C. Sanchez, R. Backov, *New Journal of Chemistry* 32 (2008) 1284.
- [18] C. Sanchez, B. Lebeau, F. Chaput, J.P. Boilot, *Advanced Materials* 15 (2003) 1969.
- [19] C. Sanchez, B. Julian, P. Belleville, M. Popall, *Journal of Materials Chemistry* 15 (2005) 3559.
- [20] F. Mammeri, E. Le Bourhis, L. Rozes, C. Sanchez, *Journal of Materials Chemistry* 15 (2005) 3787.
- [21] L. Nicole, C. Boissière, D. Grosso, A. Quach, C. Sanchez, *Journal of Materials Chemistry* 15 (2005) 3598.
- [22] L. Rozes, N. Steunou, G. Fornasieri, C. Sanchez, *Monatshefte für Chemie* 137 (2006) 501.
- [23] C.J. Brinker, G.W. Scherer, *Sol-Gel Science. The Physics and Chemistry of Sol-Gel Processing*, Academic Press, San Diego, 1990;
L.C. Klein, *Sol-Gel Technology for Thin Films, Fibers, Preforms. Electronics and Specialty Shapes*, Noyes Publications, 1988.
- [24] P. Gómez-Romero, C. Sanchez, *Functional Hybrid Materials*, Wiley-VCH, Weinheim, 2004.
- [25] D.A. Loy, K.J. Shea, *Chemical Reviews* 95 (1995) 1431;
R.J.P. Corriu, D. Leclercq, *Angewandte Chemie-International Edition* 35 (1996) 1420;
R.J.P. Corriu, *Comptes Rendus De L'Academie Des Sciences Serie Ii Fascicule C-Chimie* 1 (1998) 83.
- [26] While most sol-gel chemistry depends on the use of controlled water quantities to yield metal-oxo polymers, there is an alternative method to generate metal-oxo polymers in non-hydrolytic conditions see e.g. Bourget, L., Corriu, R.J.P., Leclercq, D., Mutin, P.H., Vioux A. J. *Non-Cryst. Solids* 1998, 242, 81 and references therein.
- [27] P. Judeinstein, C. Sanchez, *Journal of Materials Chemistry* 6 (1996) 511.
- [28] O.M. Yaghi, O.K. M, N.W. Ockwig, H.K. Chae, M. Eddaoudi, J. Kim, *Nature* 423 (2003) 705;
H. Li, M. Eddaoudi, M. O'Keeffe, O.M. Yaghi, *Nature* 402 (1999) 276;
H.K. Chae, D.Y. Siberio Perez, J. Kim, Y. Go, M. Eddaoudi, A.J. Matzger, O.K. M, O.M. Yaghi, *Nature* 427 (2004) 523;
O.M. Yaghi, G.M. Li, H.L. Li, *Nature* 378 (1995) 703;
G. Ferey, *Chemistry of Materials* 13 (2001) 3084;
G. Ferey, M. Latroche, C. Serre, F. Millange, T. Loiseau, A. Percheron-Guegan, *Chemical Communications* (2003) 2976;
F. Millange, C. Serre, J. Marrot, N. Gardant, F. Pelle, G. Ferey, *Journal of Materials Chemistry* 14 (2004) 642;

- T. Loiseau, C. Serre, C. Huguenard, G. Fink, F. Taulelle, M. Henry, T. Bataille, G. Ferey, *Chemistry-A European Journal* 10 (2004) 1373;
- C. Serre, F. Millange, S. Surble, G. Ferey, *Angewandte Chemie-International Edition* 43 (2004) 6286;
- G. Ferey, C. Serre, C. Mellot-Drazniéks, F. Millange, S. Surble, J. Dutour, I. Margiolaki, *Angewandte Chemie-International Edition* 43 (2004) 6296;
- G. Ferey, C. Mellot-Drazniéks, C. Serre, F. Millange, *Accounts of Chemical Research* 38 (2005) 217;
- A.K. Cheetham, C.N.R. Rao, *MRS Bulletin* 30 (2005) 93.
- [29] E. Bourgeat-Lamy, *Journal of Nanosciences and Nanotechnologies* 2 (2002) 1.
- [30] E. Ruiz-Hitzky, *Advanced Materials* 5 (1993) 334;
- R.A. Vaia, E.P. Giannelis, *MRS Bulletin* 26 (2001) 394;
- E.P. Giannelis, *Applied Organometallic Chemistry* 12 (1998) 675;
- F. Leroux, J.P. Besse, *Actualite Chimique* (2004) 23;
- F. Leroux, J.P. Besse, *Chemistry of Materials* 13 (2001) 3507;
- V. Prevot, C. Forano, J.P. Besse, *Applied Clay Science* 18 (2001) 3.
- [31] F. Schuth, *Chemistry of Materials* 13 (2001) 3184;
- C.T. Kresge, M.E. Leonowicz, W.J. Roth, J.C. Vartuli, J.S. Beck, *Nature* 359 (1992) 710;
- A. Stein, B.J. Melde, R.C. Schroden, *Advanced Materials* 12 (2000) 1403.
- [32] K.J.C. van Bommel, A. Friggeri, S. Shinkai, *Angewandte Chemie-International Edition* 42 (2003) 980.
- [33] Y. Sakatani, C. Boissiere, D. Grosso, L. Nicole, G. Soler-Illia, C. Sanchez, *Chemistry of Materials* 20 (2008) 1049.
- [34] M. Llusar, C. Sanchez, *Chemistry of Materials* 20 (2008) 782.
- [35] U.H.F. Bunz, *Advanced Materials* 18 (2006) 973.
- [36] C. Sanchez, G.J.A.A. Soler-Illia, F. Ribot, D. Grosso, *Comptes Rendus Chimie* 6 (2003) 1131.
- [37] B. Arkles, *MRS Bulletin* 26 (2001) 402.
- [38] T. Itou, H. Matsuda, *Key Engineering Materials* 67 (1998) 150.
- [39] G. Schottner, *Chemistry of Materials* 13 (2001) 3422.
- [40] M.T. Reetz, *Advanced Materials* 9 (1997) 943.
- [41] Dittmar, G. Delhomme, *Les systèmes vivants : une source d'inspiration pour les microsystèmes*, in: T.e.D.E. OFTA (Ed.), *Microsystèmes Arago* 21, 1999, pp. 123;
- J. Vincent, *Structural biomaterials and biomimetic strategies*, Paris, 2001;
- J.F.V. Vincent, *Structural biomaterials*, Princeton University Press, 1990.
- [42] G. Kicckelbick, *Hybrid Materials*, Wiley-VCH, Weinheim, 2006.
- [43] E. Ruiz Hitzky, K. Ariga, Y.M. Lvov, *Bio-inorganic Hybrid Nanomaterials: Strategies, Syntheses, Characterization and Applications*, Wiley-VCH, 2007;
- T. Coradin, N. Nassif, J. Livage, *Applied Microbiology and Biotechnology* 61 (2003) 429;
- T. Coradin, P.J. Lopez, *Chembiochem* 4 (2003) 251;
- T. Coradin, M. Boissière, J. Livage, *Current Medicinal Chemistry* 13 (2006) 99;
- P.J. Lopez, C. Gautier, J. Livage, T. Coradin, *Current Nanoscience* 1 (2005) 73;
- T. Coradin, J. Allouche, C. Boissière, J. Livage, *Current Nanoscience* 2 (2006) 219;
- T. Coradin, J. Livage, *Accounts of Chemical Research* 40 (2007) 819;
- J. Livage, T. Coradin, C. Roux, *Journal of Physics-Condensed Matter* 13 (2001) R673;
- T. Coradin, P.J. Lopez, C. Gautier, J. Livage, *Comptes Rendus Palevol* 3 (2004) 443.
- [44] F. Ribot, C. Sanchez, *Comments on Inorganic Chemistry* 20 (1999) 327;
- G. Kicckelbick, *Progress in Polymer Science* 28 (2003) 83.
- [45] N. Chemin, L. Rozes, C. Chaneac, S. Cassaignon, E. Le Bourhis, J.P. Jolivet, O. Spalla, E. Barthel, C. Sanchez, *Chemistry of Materials* 20 (2008) 4602.
- [46] *Hybrid plastics 2008 catalogue*.
- [47] S.H. Phillips, T.S. Haddad, S.J. Tomczak, *Current Opinion in Solid State & Materials Chemistry* 8 (2004) 21;
- R.M. Laine, *Journal of Materials Chemistry* 15 (2005) 3725;
- M.F. Roll, M.Z. Asuncion, J. Kampf, R.M. Laine, *Acs Nano* 2 (2008) 320;
- I.A. Zucchi, M.J. Galante, R.J.J. Williams, E. Franchini, J. Galy, J.F. Gerard, *Macromolecules* 40 (2007) 1274;
- J. Wu, T.S. Haddad, G.M. Kim, P.T. Mather, *Macromolecules* 40 (2007) 544.
- [48] F. Ribot, D. Veautier, S.J. Guillaudeu, T. Lalot, *Journal of Materials Chemistry* 15 (2005) 3973.
- [49] E. Martinez-Ferrero, F. Ribot, L. Rozes, C. Sanchez, L. Matejka, *Progress in Solid State Chemistry* 33 (2005) 89.
- [50] G. Fornasieri, L. Rozes, S. Le Calvé, B. Alonso, D. Massiot, M.N. Rager, M. Evain, K. Boubekeur, C. Sanchez, *Journal of the American Chemical Society* 127 (2005) 4869.
- [51] G.J.A.A. Soler-Illia, L. Rozes, M.K. Boggiano, C. Sanchez, C.O. Turrin, A.M. Caminade, J.P. Majoral, *Angewandte Chemie-International Edition* 39 (2000) 4250.
- [52] S. Le Calvé, B. Alonso, L. Rozes, C. Sanchez, M.N. Rager, D. Massiot, *Comptes Rendus Chimie* 7 (2004) 241.
- [53] L. Rozes, S. Cochet, T. Frot, G. Fornasieri, C. Sassoie, M. Popall, C. Sanchez, *Titanium oxo-clusters: versatile nano-objects for the design of hybrid compounds*, in: R.M. Laine, C. Sanchez, C. Barbé, U. Schubert, P. Warrendale (Eds.), *Organic/Inorganic Hybrid Materials in Materials Research Society Symposium Proceedings*, San Francisco, 2007, pp. S15.
- [54] E. Scolan, C. Sanchez, *Chemistry of Materials* 10 (1998) 3217;
- S. de Monredon, A. Cellot, F. Ribot, C. Sanchez, L. Armelao, L. Gueneau, L. Delattre, *Journal of Materials Chemistry* 12 (2002) 2396.
- [55] S. Roux, G. Soler-Illia, S. Demoustier-Champagne, P. Audebert, C. Sanchez, *Advanced Materials* 15 (2003) 217.
- [56] A. Perro, S. Reculosa, S. Ravaine, E.B. Bourgeat-Lami, E. Duguet, *Journal of Materials Chemistry* 15 (2005) 3745;
- R. Erhardt, A. Boker, H. Zettl, H. Kaya, W. Pyckhout-Hintzen, G. Krausch, V. Abetz, A.H.E. Mueller, *Macromolecules* 34 (2001) 1069;
- R. Erhardt, M.F. Zhang, A. Boker, H. Zettl, C. Abetz, P. Frederik, G. Krausch, V. Abetz, A.H.E. Muller, *Journal of the American Chemical Society* 125 (2003) 3260;
- R.F. Shepherd, J.C. Conrad, S.K. Rhodes, D.R. Link, M. Marquez, D.A. Weitz, J.A. Lewis, *Langmuir* 22 (2006) 8618;
- K.L. Wooley, C.J. Hawker, J.M.J. Frechet, *Journal of the American Chemical Society* 115 (1993) 11496;
- H. Xu, R. Erhardt, V. Abetz, A.H.E. Muller, W.A. Goedel, *Langmuir* 17 (2001) 6787;
- L. Nagle, D. Ryan, S. Cobbe, D. Fitzmaurice, *Nano Letters* 3 (2003) 51;
- L. Petit, E. Sellier, E. Duguet, S. Ravaine, C. Mingotaud, *Journal of Materials Chemistry* 10 (2000) 253;

- L. Petit, J.P. Manaud, C. Mingotaud, S. Ravaine, E. Duguet, *Materials Letters* 51 (2001) 478.
- [57] C. Vilain, F. Goettmann, A. Moores, P. Le Floch, C. Sanchez, *Journal of Materials Chemistry* 17 (2007) 3509.
- [58] S. Trabelsi, A. Janke, R. Hassler, N.E. Zafeiropoulos, G. Fornasieri, S. Bocchini, L. Rozes, M. Stamm, J.F. Gerard, C. Sanchez, *Macromolecules* 38 (2005) 6068; S. Bocchini, G. Fornasieri, L. Rozes, S. Trabelsi, J. Galy, N.E. Zafeiropoulos, M. Stamm, J.F. Gerard, C. Sanchez, *Chemical Communications* 20 (2005) 2600; L. Rozes, G. Fornasieri, S. Trabelsi, C. Creton, N.E. Zafeiropoulos, M. Stamm, C. Sanchez, *Progress in Solid State Chemistry* 33 (2005) 127.
- [59] P. Escribano, B. Julian-Lopez, J. Planelles-Arago, E. Cordoncillo, B. Viana, C. Sanchez, *Journal of Materials Chemistry* 18 (2008) 23.
- [60] S. Cochet, L. Rozes, M. Popall, C. Sanchez, *Materials Science & Engineering C-Biomimetic and Supramolecular Systems* 27 (2007) 1401.
- [61] O. Kameneva, A.I. Kuznestov, L.A. Smirnova, L. Rozes, C. Sanchez, A. Alexandrov, N. Bituryn, K. Chhor, A. Kanaev, *Journal of Materials Chemistry* 15 (2005) 3380.
- [62] A.I. Kuznetsov, O. Kameneva, N. Bituryn, L. Rozes, C. Sanchez, A. Kanaev, *Phys Chem Chem Phys* 11 (2009) 1248.
- [63] L. Van Lokeren, G. Maheut, F. Ribot, V. Escax, I. Verbruggen, C. Sanchez, J.C. Martins, M. Biesemans, R. Willem, *Chemistry-A European Journal* 13 (2007) 6957.
- [64] C.S. Johnson, *Progress in Nuclear Magnetic Resonance Spectroscopy* 34 (1999) 203; P. Griffiths, P. Stilbs, *Current Opinion in Colloid & Interface Science* 7 (2002) 249; P.S. Pregosin, P.G.A. Kumar, I. Fernandez, *Chemical Reviews* 105 (2005) 2977.
- [65] L. Van Lokeren, R. Kerssebaum, R. Willem, P. Denkova, *Magnetic Resonance in Chemistry* 46 (2008) S63.
- [66] R.H. Terrill, T.A. Postlethwaite, C.H. Chen, C.D. Poon, A. Terzis, A.D. Chen, J.E. Hutchison, M.R. Clark, G. Wignall, J.D. Londono, R. Superfine, M. Falvo, C.S. Johnson, E.T. Samulski, R.W. Murray, *Journal of the American Chemical Society* 117 (1995) 12537; O. Kohlmann, W.E. Steinmetz, X.A. Mao, W.P. Wuelfing, A.C. Templeton, R.W. Murray, C.S. Johnson, *Journal of Physical Chemistry B* 105 (2001) 8801.
- [67] F. Ribot, V. Escax, C. Roiland, C. Sanchez, J.C. Martins, M. Biesemans, I. Verbruggen, R. Willem, *Chemical Communications* (2005) 1019.
- [68] Z. Hens, I. Moreels, J.C. Martins, *Chemphyschem* 6 (2005) 2578.
- [69] I. Moreels, J.C. Martins, Z. Hens, *Chemphyschem* 7 (2006) 1028.
- [70] L. Shen, R. Soong, M.F. Wang, A. Lee, C. Wu, G.D. Scholes, P.M. Macdonald, M.A. Winnik, *Journal of Physical Chemistry B* 112 (2008) 1626; I. Moreels, B. Fritzing, J.C. Martins, Z. Hens, *Journal of the American Chemical Society* 130 (2008) 15081; B. Fritzing, I. Moreels, P. Lommens, R. Koole, Z. Hens, J.C. Martins, *Journal of the American Chemical Society* 131 (2009) 3024.
- [71] C.S. Johnson, *Journal of Magnetic Resonance Series A* 102 (1993) 214.
- [72] F. Guillemot, L. Van Lokeren, B. Dubertret, R. Willem, F. Ribot, *Forthcoming paper*.
- [73] F. Ribot, A. Lafuma, B.C. Eychenne, C. Sanchez, *Advanced Materials* 14 (2002) 1496.
- [74] F. Ribot, V. Escax, J.C. Martins, M. Biesemans, L. Ghys, I. Verbruggen, R. Willem, *Chemistry-A European Journal* 10 (2004) 1747.
- [75] C. Boissière, D. Grosso, H. Amenitsch, A. Gibaud, A. Coupe, N. Baccile, C. Sanchez, *Chemical Communications* (2003) 2798.
- [76] D. Grosso, C. Boissière, L. Nicole, C. Sanchez, *Journal of Sol Gel Science & Technology* 40 (2006) 141.
- [77] D. Grosso, F. Cagnol, G.J.A.A. Soler-Illia, E.L. Crepaldi, H. Amenitsch, A. Brunet-Bruneau, A. Bourgeois, C. Sanchez, *Advanced Functional Materials* 14 (2004) 309.
- [78] D. Grosso, F. Babonneau, P.A. Albouy, H. Amenitsch, A.R. Balkenende, A. Brunet Bruneau, J. Rivory, *Chemistry of Materials* 14 (2002) 931.
- [79] E.L. Crepaldi, G.J.A.A. Soler-Illia, D. Grosso, F. Cagnol, F. Ribot, C. Sanchez, *Journal of the American Chemical Society* 125 (2003) 9770.
- [80] E.L. Crepaldi, G.J.A.A. Soler-Illia, D. Grosso, P.A. Albouy, C. Sanchez, *Chemical Communications* (2001) 1582; E.L. Crepaldi, G.J.A.A. Soler-Illia, D. Grosso, M. Sanchez, *New Journal of Chemistry* 27 (2003) 9.
- [81] D. Grosso, G.J.A.A. Soler-Illia, F. Babonneau, C. Sanchez, P.A. Albouy, A. Brunet Bruneau, A.R. Balkenende, *Advanced Materials* 13 (2001) 1085.
- [82] D. Grosso, G.J.A.A. Soler-Illia, E.L. Crepaldi, F. Cagnol, C. Sinturel, A. Bourgeois, A. Brunet Bruneau, H. Amenitsch, P.A. Albouy, C. Sanchez, *Chemistry of Materials* 15 (2003) 4562.
- [83] E.L. Crepaldi, D. Grosso, G.J.A.A. Soler-Illia, P.A. Albouy, H. Amenitsch, C. Sanchez, *Chemistry of Materials* 14 (2002) 3316.
- [84] E. Crepaldi, G.J.A.A. Soler-Illia, A. Bouchara, D. Grosso, D. Durand, C. Sanchez, *Angewandte Chemie-International Edition* 42 (2003) 347.
- [85] T. Brezesinski, M. Antonietti, M. Groenewolt, N. Pinna, B. Smarsly, *New Journal of Chemistry* 29 (2005) 237.
- [86] A.B. Dros, D. Grosso, C. Boissière, G.J.A.A. Soler-Illia, P.-A. Albouy, H. Amenitsch, C. Sanchez, *Microporous & Mesoporous Materials* 94 (2006) 208.
- [87] T. Brezesinski, B. Smarsly, K. Iimura, D. Grosso, C. Boissière, H. Amenitsch, M. Antonietti, C. Sanchez, *Small* 1 (2005) 889.
- [88] T. Brezesinski, D. Fattakhova-Rohlfing, S. Sallard, M. Antonietti, B.M. Smarsly, *Small* 2 (2006) 1203.
- [89] T. Brezesinski, A. Fischer, K. Iimura, C. Sanchez, D. Grosso, M. Antonietti, B.M. Smarsly, *Advanced Functional Materials* 16 (2006) 1433.
- [90] D. Grosso, C. Boissière, B. Smarsly, T. Brezesinski, N. Pinna, P.A. Albouy, H. Amenitsch, M. Antonietti, C. Sanchez, *Nature Materials* 3 (2004) 787.
- [91] D.O. de Zarate, C. Boissière, D. Grosso, P.A. Albouy, H. Amenitsch, P. Amoros, C. Sanchez, *New Journal of Chemistry* 29 (2005) 141.
- [92] M. Kuemmel, D. Grosso, U. Boissière, B. Smarsly, T. Brezesinski, P.A. Albouy, H. Amenitsch, C. Sanchez, *Angewandte Chemie-International Edition* 44 (2005) 4589.
- [93] Y. Castro, B. Julian, C. Boissière, B. Viana, H. Amenitsch, D. Grosso, C. Sanchez, *Nanotechnology* 18 (2007).
- [94] Y. Castro, B. Julian-Lopez, C. Boissière, B. Viana, D. Grosso, C. Sanchez, *Microporous & Mesoporous Materials* 103 (2007) 273.
- [95] J.D. Bass, C. Boissière, L. Nicole, D. Grosso, C. Sanchez, *Chemistry of Materials* 20 (2008) 5550;

- J.D. Bass, D. Grosso, C. Boissiere, C. Sanchez, *Journal of the American Chemical Society* 130 (2008) 7882.
- [96] G.J.A.A. Soler-Illia, P. Innocenzi, *Chemistry-A European Journal* 12 (2006) 4478.
- [97] C.J. Brinker, D.R. Dunphy, *Current Opinion in Colloid & Interface Science* 11 (2006) 126;
K.J. Edler, Formation of Ordered Mesoporous Thin Films Through Templating, in: S. Sakka (Ed.), *Handbook of Sol-Gel Science & Technology - Processing characterization & applications*, Kluwer Academic Publisher, 2005, p. 541.
- [98] C.J. Brinker, *MRS Bulletin* 29 (2004) 631.
- [99] C.J. Brinker, Y. Lu, A. Sellinger, H. Fan, *Advanced Materials* 11 (1999) 579.
- [100] C. Sassoie, C. Laberty, C. Boissière, M. Antonietti, C. Sanchez, *Advanced Functional Materials* 19 (2009) 1922;
J. Hierso, O. Sel, A. Ringuede, C. Laberty-Robert, L. Bianchi, D. Grosso, C. Sanchez, *Chemistry of Materials* 21 (2009) 2184.
- [101] F. Hoffmann, M. Cornelius, J. Morell, M. Fröba, *Angewandte Chemie-International Edition* 45 (2006) 3216.
- [102] L. Nicole, C. Boissière, D. Grosso, P. Hesemann, J. Moreau, C. Sanchez, *Chemical Communications* (2004) 2312.
- [103] F. Cagnol, D. Grosso, C. Sanchez, *Chemical Communications* 15 (2004) 1742.
- [104] N.G. Liu, R.A. Assink, B. Smarsly, C.J. Brinker, *Chemical Communications* (2003) 1146;
X. Zhang, W.J. Wu, J.F. Wang, C.L. Liu, *Journal of the American Ceramic Society* 90 (2007) 965;
P. Innocenzi, L. Malfatti, T. Kidchob, P. Falcaro, M.C. Guidi, M. Piccinini, A. Marcelli, *Chemical Communications* (2005) 2384;
M. Ogawa, T. Kikuchi, *Advanced Materials* 10 (1998) 1077;
P. Falcaro, S. Costacurta, G. Mattei, H. Amenitsch, A. Marcelli, M.C. Guidi, M. Piccinini, A. Nucara, L. Malfatti, T. Kidchob, P. Innocenzi, *Journal of the American Chemical Society* 127 (2005) 3838;
H. Miyata, T. Suzuki, A. Fukuoka, T. Sawada, M. Watanabe, T. Noma, K. Takada, T. Mukaide, K. Kuroda, *Nature Materials* 3 (2004) 651;
S. Sugahara, T. Kadoya, K. Usami, T. Hattori, M. Matsumura, *Journal of the Electrochemical Society* 148 (2001) F120.
- [105] A. Quach, V. Escax, L. Nicole, P. Goldner, O. Guillot-Noël, P. Aschehoug, P. Hesemann, J. Moreau, D. Gourier, C. Sanchez, *Journal of Materials Chemistry* 17 (2007) 2552.
- [106] J.I. Jung, J.Y. Bae, B.S. Bae, *Journal of Materials Chemistry* 14 (2004) 1988.
- [107] L. Pido, D. Grosso, G.J.A.A. Soler-Illia, E.L. Crepaldi, C. Sanchez, P.A. Albouy, H. Amenitsch, P. Euzen, *Journal of Materials Chemistry* 12 (2002) 557.
- [108] K.N. Idrissi, A. Ayril, M. Klotz, P.A. Albouy, M.A. El, d.L.A. Van, C. Guizard, *Materials Letters* 50 (2001) 57.
- [109] N.G. Liu, R.A. Assink, C.J. Brinker, *Chemical Communications* (2003) 370;
Y. Lu, R. Ganguli, C.A. Drewien, M.T. Anderson, C.J. Brinker, W. Gong, Y. Guo, H. Soye, B. Dunn, M.H. Huang, J.I. Zink, *Nature* 389 (1997) 364.
- [110] C.Y. Chiu, A.S.T. Chiang, K.J. Chao, *Microporous & Mesoporous Materials* 91 (2006) 244.
- [111] S. Dourdain, A. Mehdi, J.F. Bardeau, A. Gibaud, *Thin Solid Films* 495 (2006) 205.
- [112] M.R. Baklanov, K.P. Mogilnikov, V.G. Polovinkin, F.N. Dultsev, *Journal of Vacuum Science & Technology B* 18 (2000) 1385.
- [113] C. Boissière, D. Grosso, S. Lepoutre, L. Nicole, A. Brunet-Bruneau, C. Sanchez, *Langmuir* 21 (2005) 12362.
- [114] A. Bourgeois, A. Brunet-Bruneau, S. Fisson, B. Demarets, D. Grosso, F. Cagnol, C. Sanchez, J. Rivory, *Thin Solid Films* 447–448 (2004) 46.
- [115] J.D. Bass, D. Grosso, C. Boissière, E. Belamie, T. Coradin, C. Sanchez, *Chemistry of Materials* 19 (2007) 4349.
- [116] M. Etienne, A. Quach, D. Grosso, L. Nicole, C. Sanchez, A. Walcarius, *Chemistry of Materials* 19 (2007) 844.
- [117] Y. Sakatani, D. Grosso, L. Nicole, C. Boissière, G.J.A.A. Soler-Illia, C. Sanchez, *Journal of Materials Chemistry* 16 (2006) 77.
- [118] E. Martinez-Ferrero, Y. Sakatani, C. Boissière, D. Grosso, A. Fuertes, J. Fraxedas, C. Sanchez, *Advanced Functional Materials* 17 (2007) 3348.
- [119] E. Lancelle-Beltran, P. Prene, C. Boscher, P. Belleville, P. Buvat, C. Sanchez, *Advanced Materials* 18 (2006) 2579.
- [120] E. Lancelle-Beltran, P. Prene, C. Boscher, P. Belleville, P. Buvat, S. Lambert, F. Guillet, C. Boissière, D. Grosso, C. Sanchez, *Chemistry of Materials* 18 (2006) 6152.
- [121] E. Martinez-Ferrero, D. Grosso, C. Boissière, C. Sanchez, O. Oms, D. Leclercq, A. Vioux, F. Miomandre, P. Audebert, *Journal of Materials Chemistry* 16 (2006) 3762.
- [122] M. Etienne, D. Grosso, C. Boissière, C. Sanchez, A. Walcarius, *Chemical Communications* (2005) 4566.
- [123] H.Y. Fan, Y.F. Lu, A. Stump, S.T. Reed, T. Baer, R. Schunk, L.V. Perez, G.P. Lopez, C.J. Brinker, *Nature* 405 (2000) 56.
- [124] H.Y. Fan, S. Reed, T. Baer, R. Schunk, G.P. Lopez, C.J. Brinker, *Microporous & Mesoporous Materials* 44 (2001) 625;
G. Wirmsberger, B.J. Scott, G.D. Stucky, *Chemical Communications* 1 (2001) 119.
- [125] B.F. Lei, B. Li, H.R. Zhang, S.Z. Lu, Z.H. Zheng, W.L. Li, Y. Wang, *Advanced Functional Materials* 16 (2006) 1883.
- [126] S.Y. Tao, G.T. Li, *Colloid & Polymer Science* 285 (2007) 721;
S.Y. Tao, G.T. Li, H.S. Zhu, *Journal of Materials Chemistry* 16 (2006) 4521.
- [127] P. Banet, L. Legagneux, P. Hesemann, J. Moreau, L. Nicole, A. Quach, C. Sanchez, T.-H. Tran-Thi, *Sensors & Actuators B: Chemical* 130 (2008) 1.
- [128] N. Stevens, D.L. Akins, *Sensors & Actuators B: Chemical* 123 (2007) 59.
- [129] O.B. Miled, D. Grosso, C. Sanchez, J. Livage, *Journal of Physics & Chemistry of Solids* 65 (2004) 1751.
- [130] O.B. Miled, C. Boissière, C. Sanchez, J. Livage, *Journal of Physics & Chemistry of Solids* 67 (2006) 1775;
O.B. Miled, C. Sanchez, J. Livage, *Journal of Materials Science* 40 (2005) 4523.
- [131] F. Goettmann, A. Moores, C. Boissière, P. Le Floch, C. Sanchez, *Small* 1 (2005) 636;
F. Goettmann, A. Moores, C. Boissière, P. Le Floch, C. Sanchez, *Thin Solid Films* 495 (2006) 280.
- [132] M.C. Fuertes, F.J. López-Alcaraz, M.C. Marchi, H.E. Troiani, V. Luca, H. Míguez, G.J.A.A. Soler-Illia, *Advanced Functional Materials* 17 (2007) 1247.
- [133] S.Y. Choi, M. Mamak, G. vonFreyman, N. Chopra, G.A. Ozin, *Nano Letters* 6 (2006) 2456.
- [134] K. Valle, P. Belleville, F. Pereira, C. Sanchez, *Nature Materials* 5 (2006) 107.
- [135] O. Sel, C. Laberty-Robert, T. Azais, C. Sanchez, *Physical Chemistry Chemical Physics* 11 (2009) 3733.
- [136] F. Pereira, K. Valle, P. Belleville, A. Morin, S. Lambert, C. Sanchez, *Chemistry of Materials* 20 (2008) 1710.

- [137] A. Fisher, M. Kuemmel, M. Jarn, M. Linden, C. Boissiere, L. Nicole, C. Sanchez, D. Grosso, *Small* 2 (2006) 569.
- [138] M. Kuemmel, C. Boissiere, L. Nicole, C. Laberty-Robert, C. Sanchez, D. Grosso, *Journal of Sol-Gel Science and Technology* 48 (2008) 102.
- [139] M. Kuemmel, J. Allouche, L. Nicole, C. Boissiere, C. Laberty, H. Amenitsch, C. Sanchez, D. Grosso, *Chemistry of Materials* 19 (2007) 3717.
- [140] M. Kuemmel, J.-H. Smatt, C. Boissiere, L. Nicole, C. Sanchez, M. Linden, D. Grosso, *Journal of Materials Chemistry* 19 (2009) 3638.
- [141] C. Laberty-Robert, M. Kuemmel, J. Allouche, C. Boissiere, L. Nicole, D. Grosso, C. Sanchez, *Journal of Materials Chemistry* 18 (2008) 1216.
- [142] M. Jarn, F.J. Brieler, M. Kuemmel, D. Grosso, M. Linden, *Chemistry of Materials* 20 (2008) 1476.
- [143] D.A. Olson, L. Chen, M.A. Hillmyer, *Chemistry of Materials* 20 (2008) 869.
- [144] Y. Lu, H. Fan, A. Stump, T.L. Ward, T. Rieker, C.J. Brinker, *Nature* 398 (1999) 223.
- [145] N. Baccile, D. Grosso, C. Sanchez, *Journal of Materials Chemistry* 13 (2003) 3011.
- [146] M.T. Bore, S.B. Rathod, T.L. Ward, A.K. Datye, *Langmuir* 19 (2003) 256.
- [147] C. Boissière, L. Nicole, C. Gervais, F. Babonneau, M. Antonietti, H. Amenitsch, C. Sanchez, D. Grosso, *Chemistry of Materials* 18 (2006) 5238.
- [148] D. Grosso, G. Illia, E.L. Crepaldi, B. Charleux, C. Sanchez, *Advanced Functional Materials* 13 (2003) 37.
- [149] Y. Yang, Y.F. Lu, M.C. Lu, J.M. Huang, R. Haddad, G. Xomeritakis, N.G. Liu, A.P. Malanoski, D. Sturmayer, H.Y. Fan, D.Y. Sasaki, R.A. Assink, J.A. Shelnut, S.F. van, G.P. Lopez, A.R. Burns, C.J. Brinker, *Journal of the American Chemical Society* 125 (2003) 1269; J.E. Hampsey, S. Arsenault, Q.Y. Hu, Y.F. Lu, *Chemistry of Materials* 17 (2005) 2475.
- [150] M.T. Bore, R.F. Marzke, T.L. Ward, A.K. Datye, *Journal of Materials Chemistry* 15 (2005) 5022; C. Coelho, T. Azaïs, G. Laurent, L. Bonhomme-Coury, C. Boissière, C. Sanchez, F. Babonneau, C. Bonhomme, submitted.
- [151] F. Goettmann, C. Boissière, D. Grosso, F. Mercier, P. Le Floch, C. Sanchez, *Chemistry-A European Journal* 11 (2005) 7416.
- [152] S. Pega, A. Coupe, C. Boissiere, T. Azaïs, D. Grosso, C. Sanchez, J. Blanchard, D. Massiot, A. Chaumonnot, *Nanoporous Materials V, Vancouver, 2008*, pp. 457.
- [153] S. Pega, C. Boissière, D. Grosso, T. Azaïs, A. Chaumonnot, C. Sanchez, *Angewandte Chemie-International Edition* 48 (2009) 2784.
- [154] S. Areva, C. Boissiere, D. Grosso, T. Asakawa, C. Sanchez, M. Linden, *Chemical Communications* (2004) 1630.
- [155] N. Baccile, A. Fischer, B. Julian-Lopez, D. Grosso, C. Sanchez, *Journal of Sol-Gel Science and Technology* 47 (2008) 119.
- [156] C.K. Tsung, J. Fan, N.F. Zheng, Q.H. Shi, A.J. Forman, J.F. Wang, G.D. Stucky, *Angewandte Chemie-International Edition* 47 (2008) 8682.
- [157] B. Julian Lopez, C. Boissière, C. Chaneac, D. Grosso, S. Vasseur, S. Miraux, E. Duguet, C. Sanchez, *Journal of Materials Chemistry* 17 (2007) 1563.
- [158] A.K. Gupta, M. Gupta, *Biomaterials* 26 (2005) 3995; S. Mornet, S. Vasseur, F. Gasset, E. Duguet, *Journal of Materials Chemistry* 14 (2004) 2161.
- [159] K. Nakanishi, *Journal of Porous Materials* 4 (1997) 67.
- [160] A. Ibanez, S. Maximov, A. Guin, C. Chaillout, P.L. Baldeck, *Advanced Materials* 10 (1998) 1540; M. Antonietti, B. Berton, C. Goltner, H.P. Hentze, *Advanced Materials* 10 (1998) 154; H. Yang, G.A. Ozin, C.T. Kresge, *Advanced Materials* 10 (1998) 883; S.M. Yang, I. Sokolov, N. Coombs, C.T. Kresge, G.A. Ozin, *Advanced Materials* 11 (1999) 1427; M. Trau, N. Yao, E. Kim, Y. Xia, G.M. Whitesides, I.A. Aksay, *Nature* 390 (1997) 674; L.M. Huang, Z.B. Wang, J.Y. Sun, L. Miao, Q.Z. Li, Y.S. Yan, D.Y. Zhao, *Journal of the American Chemical Society* 122 (2000) 3530; S.A. Davis, S.L. Burkett, N.H. Mendelson, S. Mann, *Nature* 385 (1997) 420; F. Caruso, *Advanced Materials* 13 (2001) 11.
- [161] P.D. Yang, T. Deng, D.Y. Zhao, P.Y. Feng, D. Pine, B.F. Chmelka, G.M. Whitesides, G.D. Stucky, *Science* 282 (1998) 2244.
- [162] Z.Y. Yuan, T.Z. Ren, B.L. Su, *Advanced Materials* 15 (2003) 1462; F. Xu, P. Zhang, A. Navrotsky, Z.Y. Yuan, T.Z. Ren, M. Halasa, B.L. Su, *Chemistry of Materials* 19 (2007) 5680; A. Vantomme, A. Leonard, Z.Y. Yuan, B.L. Su, *Colloids & Surfaces A: Physicochemical & Engineering Aspects* 300 (2007) 70.
- [163] M. Mougnot, M. Lejeune, J.F. Baumard, C. Boissière, F. Ribot, D. Grosso, C. Sanchez, R. Noguera, *Journal of the American Ceramic Society* 89 (2006) 1876.
- [164] N. Brun, B. Julian-Lopez, P. Hesemann, G. Laurent, H. Deleuze, C. Sanchez, M.F. Achard, R. Backov, *Chemistry of Materials* 20 (2008) 7117.
- [165] M.C. Fuentes, S. Colodrero, G. Lozano, A.R. Gonzalez-Elipe, D. Grosso, C. Boissiere, C. Sanchez, G. Soler-Illia, H. Miguez, *Journal of Physical Chemistry C* 112 (2008) 3157.
- [166] F. Audoin, H. Blas, P. Pasetto, P. Beaunier, C. Boissière, C. Sanchez, M. Save, B. Charleux, *Macromolecular Rapid Communications* 29 (2008) 914.
- [167] A. Bouchara, G. Mosser, G.J.A.A. Soler-Illia, J.Y. Chane-Ching, C. Sanchez, *Journal of Materials Chemistry* 14 (2004) 2347.
- [168] M. Save, G. Granvorka, J. Bernard, B. Charleux, C. Boissière, D. Grosso, C. Sanchez, *Macromolecular Rapid Communications* 27 (2006) 393; H. Blas, M. Save, P. Pasetto, C. Boissière, C. Sanchez, B. Charleux, *Langmuir* 24 (2008) 13132; P. Pasetto, H. Blas, F. Audoin, C. Boissière, C. Sanchez, M. Save, B. Charleux, *Macromolecules*, in press.
- [169] A. Bouchara, G.J.A.A. Soler-Illia, J.Y. Chane-Ching, C. Sanchez, *Chemical Communications* (2002) 1234.
- [170] B. de Boer, U. Stalmach, H. Nijland, G. Hadziioannou, *Advanced Materials* 12 (2000) 1581; T. Nishikawa, J. Nishida, R. Ookura, S.I. Nishimura, S. Wada, T. Karino, M. Shimomura, *Materials Science & Engineering C-Biomimetic and Supramolecular Systems* 10 (1999) 141; N. Maruyama, T. Koito, J. Nishida, T. Sawadaishi, X. Cieren, K. Ijiri, O. Karthaus, M. Shimomura, *Thin Solid Films* 327 (1997) 854.
- [171] Y. Ono, K. Nakashima, M. Sano, Y. Kanekiyo, K. Inoue, J. Hojo, S. Shinkai, *Chemical Communications* (1998) 1477; Y. Ono, K. Nakashima, M. Sano, J. Hojo, S. Shinkai, *Chemistry Letters* (1999) 1119;

- J.H. Jung, Y. Ono, S. Shinkai, *Angewandte Chemie-International Edition* 39 (2000) 1862.
- [172] G.M. Clavier, J.L. Pozzo, H. Bouas-Laurent, C. Liere, C. Roux, C. Sanchez, *Journal of Materials Chemistry* 10 (2000) 1725; M. Llusar, L. Pido, C. Roux, J.L. Pozzo, C. Sanchez, *Chemistry of Materials* 14 (2002) 5124.
- [173] M. Llusar, G. Monros, J.L. Pozzo, C. Roux, C. Sanchez, *Zeitschrift für anorganische und allgemeine Chemie* 631 (2005) 2215; M. Llusar, G. Monros, C. Roux, J.L. Pozzo, C. Sanchez, *Journal of Materials Chemistry* 13 (2003) 2505; M. Llusar, C. Roux, J.L. Pozzo, C. Sanchez, *Journal of Materials Chemistry* 13 (2003) 442.
- [174] G. Roy, J.F. Miravet, B. Escuder, C. Sanchez, M. Llusar, *Journal of Materials Chemistry* 16 (2006) 1817.
- [175] A. Stein, *Microporous & Mesoporous Materials* 44–45 (2001) 227; B. Lebeau, C.E. Fowler, S. Mann, C. Farcet, B. Charleux, C. Sanchez, *Journal of Materials Chemistry* 10 (2000) 2105; J. Wijnhoven, W.L. Vos, *Science* 281 (1998) 802; S.M. Yang, N. Coombs, G.A. Ozin, *Advanced Materials* 12 (2000) 1940; P. Jiang, J.F. Bertone, V.L. Colvin, *Science* 291 (2001) 453.
- [176] A. Imhof, D.J. Pine, *Nature* 389 (1997) 948.
- [177] Y.F. Lu, B.F. McCaughey, D.H. Wang, J.E. Hampsey, N. Doke, Z.Z. Yang, C.J. Brinker, *Advanced Materials* 15 (2003) 1733; P. Innocenzi, T. Kidchob, P. Falcaro, M. Takahashi, *Chemistry of Materials* 20 (2008) 607; J.B. Pang, J.N. Stuecker, Y.B. Jiang, A.J. Bhakta, E.D. Branson, P. Li, J. Cesarano, D. Sutton, P. Calvert, C.J. Brinker, *Small* 4 (2008) 982.
- [178] R. Noguera, C. Dossou-Yovo, M. Lejeune, T. Chartier, *Journal de Physique IV* 126 (2005) 133; R. Noguera, C. Dossou-Yovo, M. Lejeune, T. Chartier, *Journal de Physique IV* 128 (2005) 87; R. Noguera, M. Lejeune, T. Chartier, *Journal of the European Ceramic Society* 25 (2005) 2055; G. Senlis, M. Dubarry, M. Lejeune, T. Chartier, *Ferroelectrics* 273 (2002) 2657.
- [179] B. Fousseret, M. Mougenot, F. Rossignol, J.-F. Baumard, B. Soulestin, C. Boissière, F. Ribot, D. Jalabert, C. Sanchez, M. Lejeune, submitted.
- [180] D. Grosso, C. Boissière, C. Sanchez, *Nature Materials* 6 (2007) 572.
- [181] G.R. Yi, S.M. Yang, *Chemistry of Materials* 11 (1999) 2322; B.P. Binks, *Advanced Materials* 14 (2002) 1824.
- [182] F. Carn, M.F. Achard, O. Babot, H. Deleuze, S. Reculosa, R. Backov, *Journal of Materials Chemistry* 15 (2005) 3887; F. Carn, A. Colin, M.F. Achard, H. Deleuze, Z. Saadi, R. Backov, *Advanced Materials* 16 (2004) 140; F. Carn, A. Colin, M.F. Achard, H. Deleuze, C. Sanchez, R. Backov, *Advanced Materials* 17 (2005) 62; F. Carn, H. Saadaoui, P. Masse, S. Ravaine, B. Julian-Lopez, C. Sanchez, H. Deleuze, D.R. Talham, R. Backov, *Langmuir* 22 (2006) 5469; F. Carn, N. Steunou, J. Livage, A. Colin, R. Backov, *Chemistry of Materials* 17 (2005) 644.
- [183] S. Ungureanu, H. Deleuze, C. Sanchez, M.I. Popa, R. Backov, *Chemistry of Materials* 20 (2008) 6494; S. Ungureanu, M. Birot, G. Laurent, H. Deleuze, O. Babot, B. Julian-Lopez, M.F. Achard, M.I. Popa, C. Sanchez, R. Backov, *Chemistry of Materials* 19 (2007) 5786.
- [184] H.F. Zhang, A.I. Cooper, *Soft Matter* 1 (2005) 107; N.R. Cameron, *Polymer* 46 (2005) 1439; N.R. Cameron, D.C. Sherrington, High internal phase emulsions (HIPEs): Structure, properties and use in polymer preparation, *Advances in Polymer Science*, Springer, Berlin/Heidelberg, 1996, p. 163; D. Barby, H. Zia, (1982) Patent EP0060138.
- [185] R. Backov, C. Sanchez, H. Deleuze, S. Ungureanu, (2008) Patent WO2008129151; N. Brun, C. Sanchez, G. Pécastaing, A. Derré, A. Soum, H. Deleuze, M. Birot, A. Babeau, O. Babot, R. Backov, *Advanced Functional Materials*, in press.
- [186] R. Backov, *Actualite Chimique* (2009) III.